MASTER´S THESIS

Yongbo Wang 2009

LAPPEENRANTA UNIVERSITY OF TECHNOLOGY
Department of Mechanical Engineering

MASTER'S THESIS

Error Modeling and Accuracy Analysis of a Novel Mobile Hybrid Parallel Robot

The Mechanical Engineering Department council has approved the subject of this Master's thesis on 11.03.2009

Examiner: Professor Heikki Handroos
Second Examiner: Professor Huapeng Wu

Lappeenranta 25.02.2009

Yongbo Wang
Punkkerikatu 5 C52
53850 Lappeenranta
046-8977194

ABSTRACT

Author: Yongbo Wang

Name of the Master's thesis: Error Modeling and Accuracy Analysis of a Novel Mobile Hybrid Parallel Robot

Department: Mechanical Engineering

Year: 2009 **Place:** Lappeenranta University of Technology

Master's thesis. Lappeenranta University of Technology
68 pages, 38 figures, 1 table
Supervisor. Professor Heikki Handroos and Professor Huapeng Wu

Keywords: accuracy analysis, error modeling, parallel robot, kinematics analysis

Over the last decades, calibration techniques have been widely used to improve the accuracy of robots and machine tools since they only involve software modification instead of changing the design and manufacture of the hardware. Traditionally, there are four steps are required for a calibration, i.e. error modeling, measurement, parameter identification and compensation. The objective of this thesis is to propose a method for the kinematics analysis and error modeling of a newly developed hybrid redundant robot IWR (Intersector Welding Robot), which possesses ten degrees of freedom (DOF) where 6-DOF in parallel and additional 4-DOF in serial. In this article, the problem of kinematics modeling and error modeling of the proposed IWR robot are discussed. Based on the vector arithmetic method, the kinematics model and the sensitivity model of the end-effector subject to the structure parameters is derived and analyzed. The relations between the pose (position and orientation) accuracy and manufacturing tolerances, actuation errors, and connection errors are formulated. Computer simulation is performed to examine the validity and effectiveness of the proposed method.

ACKNOWLEDGMENTS

First and for most, I would like to express my deepest gratitude to my supervisor professor Heikki Handroos and my thesis advisor Huapeng Wu for their inspiring guidance, encouragement and suggestions during the writing process of this thesis and throughout this research.

Furthermore, I would like to thank the members of the Institute of Mechatronics and Virtual Engineering at LUT for their various technical contributions and advice.

The financial support from the European communities under the contract of association between EURATOM and Finnish Tekes is also acknowledged.

Last but not least, I would also like to thank my family and friends for their support throughout the studies.

Yongbo Wang
February, 2009
Lappeenranta, Finland

TABLE OF CONTENTS

1 INTRODUCTION

Accuracy is an utmost important consideration factor when design a robot, whatever it is a serial robot or a parallel one. The inaccuracy of a robot may originate from a number of error sources such as the dimensional tolerances of joint actuators and controllers, manufacturing and assembly errors, different types of measurement and control errors, and non-geometric errors such as elastic deformations of structural components of robots. As a matter of fact, all these errors are uncertain in nature, and a suitable model has to be used for predicting the performance of the robot. A common way to improve the accuracy of a given manipulator is through hardware modification, i.e. revising the robot mechanical structure or design (by proposing, for example, new joint concepts) and imposing tighter tolerances in manufacturing the robot parts. However, the manufacturing costs associated with this solution will be very high if the accuracy requirements are beyond certain levels.

It has been acknowledged that a more cost-effective solution is to build a manipulator with relaxed tolerances and to modify the mathematical model in the controller so that the software compensates for the actual inaccuracy of the robot. Robot calibration is the process of enhancing the accuracy of a given manipulator through software modification.

It is believed that parallel robot have some favorable advantages, such as higher speeds and accelerations, compact structure, and improved accuracy since the joint errors are not accumulated like in its counterpart. On the other hand, serial robots have some advantages like larger workspace, higher dexterity and good maneuverability but exhibit low stiffness and poor positioning accuracy because of their serial structures. To take advantage both of their merits, in this paper, a redundant hybrid robot which possesses both serial and parallel links will be introduced, the serial part of the machine is used to enlarge the work volume, while the parallel links bring high loading capabilities and

stiffness to the whole structure, thus a promising compromise of best sides of parallel kinematics and serial robots might be achieved.

This work will be focused on the static and load-invariant calibration of the proposed hybrid robot. In the paper, based on the differentiation algorithm method, the error model of the proposed robot will be formulated and the relative computer simulation will be performed.

1.1 Background and motivation

The motivation of this work is originated from a newly developed hybrid redundant robot IWR (Intersector Welding Robot) built in the Institute of Mechatronics and Virtual Engineering at Lappeenranta University of Technology (LUT). IWR is a hybrid robot which can be used for assembling and repairing the VV (Vacuum Vessel) of ITER (International Thermonuclear Experimental Reactor). Traditional industrial robots that have been used as general-purpose positioning devices are open chain mechanisms that generally have the links actuated in series. These kinds of manipulators are more suitable for long reach and large workspace, but are inherently not very rigid and have poor dynamic performance at high speed and high dynamic loading under operating conditions. Since commercially available machines are too heavy for the required machining operations and the lifting of a possible e-beam gun column system, a flexible, lightweight and mobile robotic machine is needed. Figure1 and Figure2 illustrate the experimental prototype of IWR for testing the cutting, welding with VVPSM (Vacuum Vessel Poloidal Segment Mock-up). Firstly, the robot carries the cutting tool to cut VVPSM into two parts, then, a splice plate is inserted into the gap between the separate parts. Then, by using narrow gap TIG (Tungsten Inert Gas) welding and laser welding splice plates are joined to the separate parts of VVPSM [1].

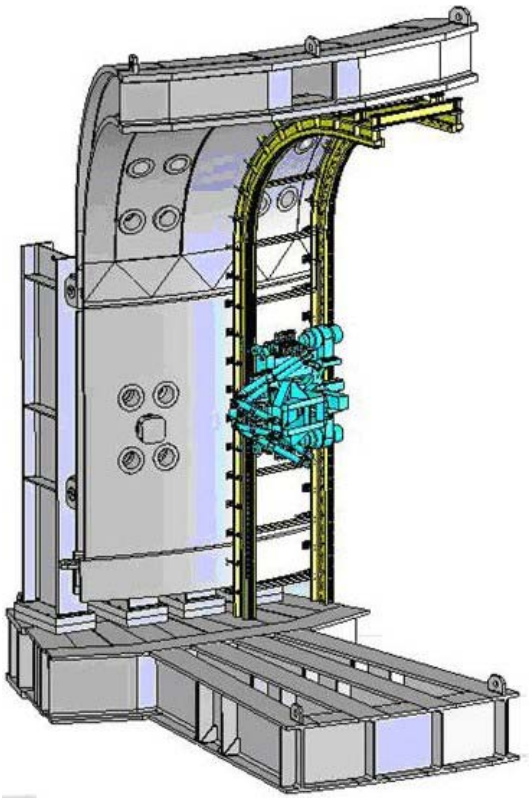

Figure 1. The 3D model of IWR moving along the rail

Figure 2. The experimental prototype developed in LUT

The word “ITER” in Latin means “the way”. The ITER experiment is a joint international research and development project that aims to demonstrate the scientific and technological feasibility of fusion energy for peaceful purposes. The aim of ITER is to show fusion could be used to generate electrical power, and to gain the necessary data to design and operate the first electricity-producing plant. The long-term objective of fusion research is to harness the nuclear energy provided by the fusion of light atoms to help meet mankind’s future energy needs. This research, which is carried out by scientists from all over the world, the partners in the project – the ITER Parties or Members – are the European Union (represented by EURATOM), Japan, the People’s Republic of China, India, the Republic of Korea, the Russian Federation and the USA [2].

The ITER machine is shown in Figure3. The Vacuum Vessel of ITER consists of nine sectors which require more stringent tolerances than normally expected for the size of structure. The inner and outer walls of the ITER Vacuum Vessel are made of 60mm thick stainless steel 316L and are welded together by high efficiency structural and leak-tight welds. In addition to the initial Vacuum Vessel assembly, sectors may have to be replaced for repair. Sectors are not welded together directly but with an intermediate so-called “splice-plate” inserted between sectors to be joined. The splice-plate has two important functions: to allow access to bolt together the thermal shield between the Vacuum vessel and coils, and to compensate for mismatch between adjacent sectors to give a good fit-up of the sector-sector butt weld. The assembly or repair will be performed according to four steps: cutting, edge machining and smoothing, welding and NDT control. The IWR is used as a transport device for welding, machining and inspection end-effectors for ITER [1].

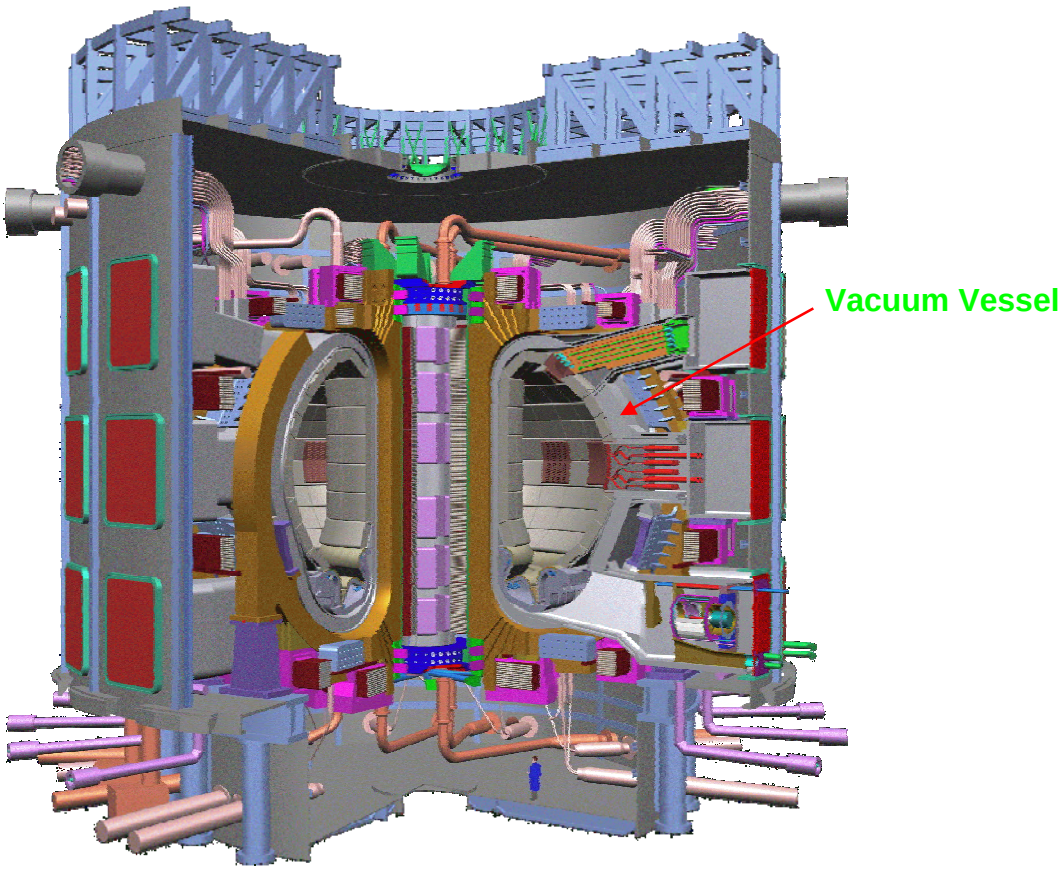

Figure 3. The ITER machine. The man in the bottom shows the scale

To satisfy the stringent accuracy requirement of ITER, the calibration of the robot has to be carried out in a laboratory before it is brought into its work environment. This work will concentrate on the development of an error model of IWR to compensate the inaccuracy caused by the manufacture errors and assembly errors.

1.2 Literature review

Robot accuracy is largely dependent on how closely the robot can be manufactured of its specifications at a minimum tolerance. Important specifications include the precise geometrical arrangement of a robot's joint-axes and the transmission mechanisms used to actuate each joint. However, after a robot is completely manufactured and assembled, many of its physical features (parameters) which represent these specifications can not

easily and explicitly be measured. Robot calibration, on the other hand, provides a practical and effective means of implicit parameter measurement. Due to the manufacturing tolerances, actuation errors and assembly errors, the actual values of the structural parameters will deviate from the nominal ones, and then the inaccuracy of robot is inevitable. It has been shown that as much as 95% of robot positioning inaccuracy arises from the inaccuracy in its kinematics model description [3]. The techniques of kinematics calibration can be used to improve robot accuracy through modifying the control software without changing the mechanical structure or design of the robot. Calibration can also be used to minimize the risk of having to change application programs due to slight changes or drifts, such as wear of parts, dimensional drifts and tolerances and component replacement effects in the robot system. This is especially important for the applications that may involve a rather large number of task points.

At a most general level, robot calibration can be classified into two types [4], i.e. static calibration and dynamic calibration. From Figure 4 we can see that static calibration is an identification of those parameters which influence primarily the static (time invariant) positioning characteristics of a manipulator, whereas dynamic calibration is used to identify parameters influencing primarily motion characteristics of the manipulator (forces, actuator torques, accelerations) and dynamic effects that occur on a manipulator such as friction and link stiffness.

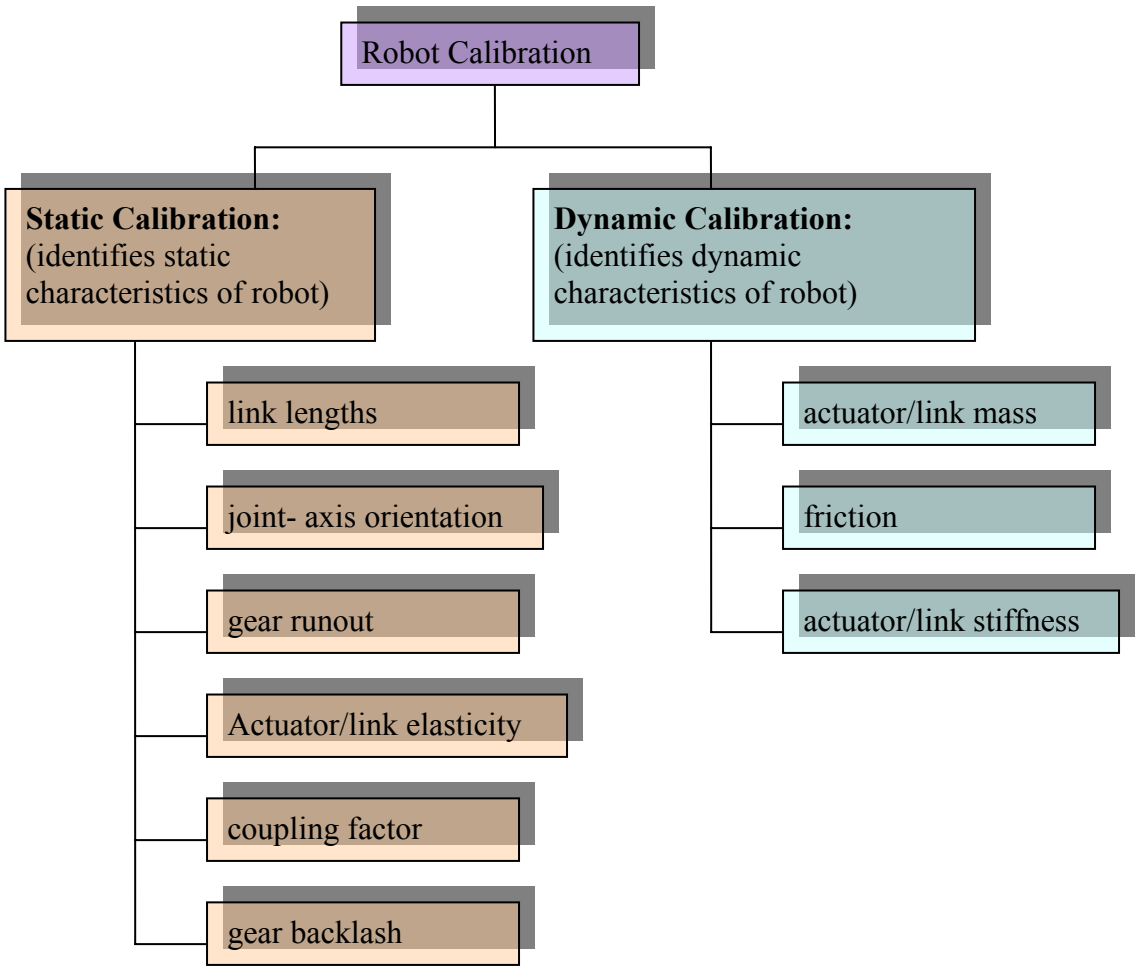

Figure 4. Diagram of robot calibration types

A static calibration procedure is used to identify the actual internal robot features such as joint-axis geometries, joint angle off-sets, and actuator/link compliances, actuator transmission and coupling factors, and gear eccentricities. All these features can have an influence to some degree on the static positioning accuracy of the robot.

Once a robot's static parameters are identified, a dynamic calibration can take place. This type of calibration is performed to determine dynamic related characteristics of the robot (e.g. distribution of mass in the links, friction in actuators and joints, stiffness, etc.).

Internal characteristics such as friction tend to be parameters difficult to identify accurately owing to their coupling with other dynamic parameters.
In what follows, the sources of inaccuracy and the robot calibration procedures and relative methods will be reviewed separately.

1.2.1 Error sources

Generally, the error sources can be classified into two different kinds according to the current literatures, i.e. the geometric and non-geometric geometric errors (or sometimes kinematic and non-kinematic). Among these literatures, most of them are focused on the static sources of inaccuracy.

Geometric errors are deviations that are constant for all robot configurations. It is well known that, due to manufacturing tolerances, the geometry of robotic manipulators does not match exactly the design goals. This may cause, for example, small changes in the link lengths of the robot which, in turn, cause positional changes of the robot end-effector. Moreover, geometric errors can also come from the assembly of the different robot components (e.g. misalignments between joint axes). Since these errors have a systematic nature, they can be compensated by means of proper modifications of the kinematic model and through a calibration procedure.

Non-geometric errors are dependent on the robot configurations. Errors occurring in the motion transmission between the different joints, such as friction, environment temperature, wear and backlash are the ones most commonly cited in the literature. Additionally, deflections in robot links may also be a source of errors. Non-geometric effects can also be at the joint level (e.g. electrical zeroes of the joint encoders do not generally coincide with the mechanical zeroes of the joints themselves) or in the control procedure (e.g. finite resolution of joint encoders, steady-state control errors).

Errors in geometric parameters are claimed to contribute most positional inaccuracy [5]. Although less significant, the positional error of non-geometric effects cannot be neglected if high positional accuracy is required. In non-geometric calibration, a number of effects exist which may be modeled. To include such factors, the model used in the position control software of the robot must be modified. On the other hand, if the robot is under dynamic control, then factors such as translational and angular velocity and acceleration of the end-effector must be considered in the functional relationship. Of course, this will complicate the functional relationship equation, even if the links of the robot assumed to be perfectly rigid and the joints are frictionless. A schematic list of the different sources of inaccuracy mentioned above is shown in Figure 5.

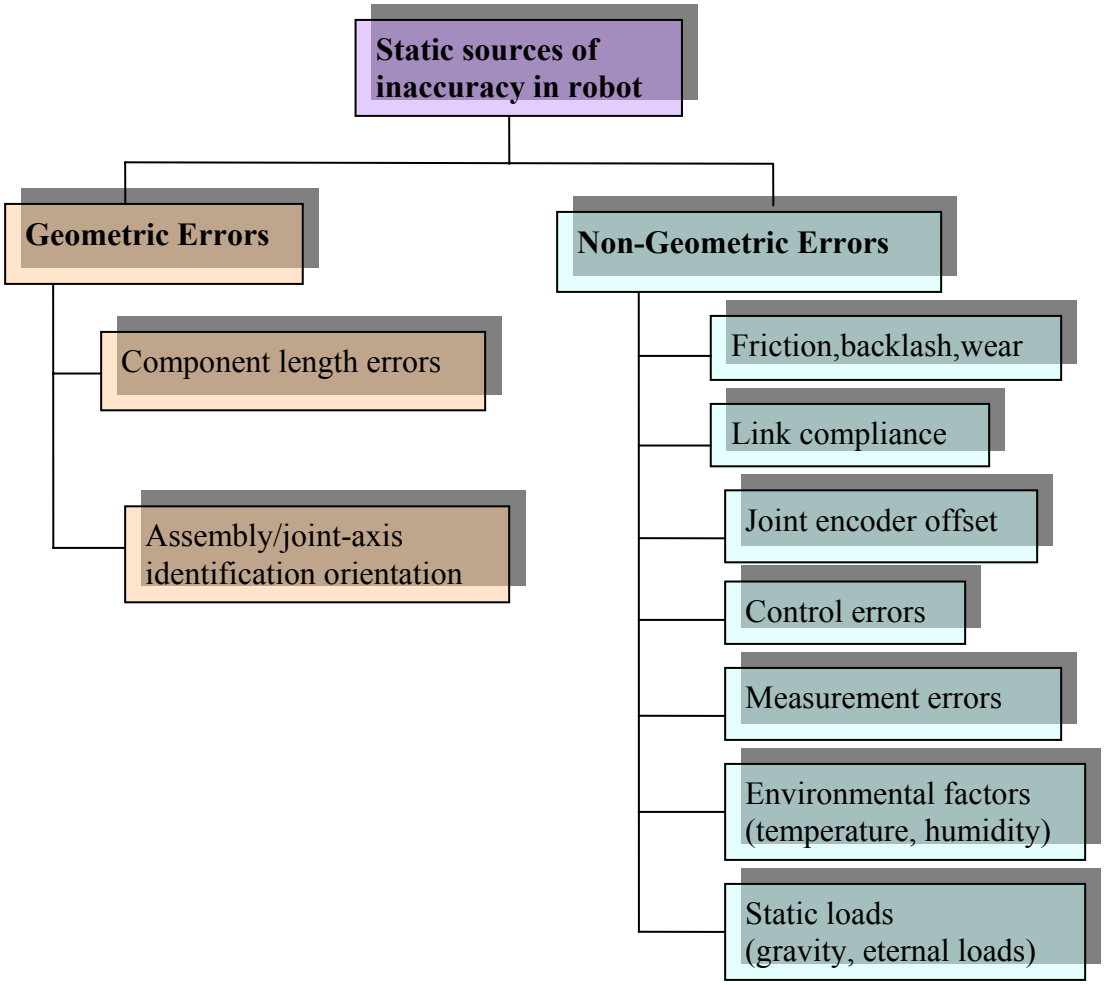

Figure 5. Sources of inaccuracy commonly considerated in static robot calibration problems

1.2.2 Steps in a calibration procedure

Robot calibration techniques are designed to improve the software model of the robot so that it is able to more closely represent the behavior of the actual robot. These techniques can be classified into two types either static or dynamic calibration. The largest body of research into static robot calibration is based on parametric models, which are designed to represent the true relationship between joint configurations and end-effector poses. Most work in this field has been conducted on forward calibration methods where calibration is applied to the forward kinematics model.

The calibration process is typically carried out using following four steps:

1) Development of a suitable model based on prior engineering knowledge, which provides a model structure and nominal parameter values (*Kinematics Modeling*).
2) Measurement of the actual position through a set of end-effector locations that relate the input of the model to the output (*Pose Measurement*).
3) The identification of the model parameters based on the collected data by using a numerical method (*Kinematics Identification*).
4) The implementation of the identified model in the position control software of the robot (*Kinematics compensation*).

In what follows, the steps will be described in detail:

1.2.2.1 Kinematics Modeling

The desired locations of a robot end-effector are normally specified in Cartesian space, while these locations are achieved by controlling the joint variables in the robot's joint space. The purpose of a geometric model is to relate the joint displacements to the pose of the end-effector. The absolute accuracy of the robot depends of course on how accurately this model reflects the actual robot. For a given set of joint coordinates, the direct (or forward) model consists of solving the geometric model for the corresponding

set of end-effector coordinates, whereas the inverse model gives, for a given set of end-effector coordinates, the corresponding joint coordinates.

The goal of calibration is to replace these nominal models by a more accurate description of the relationship between joint and end-effector coordinates. Different types of approaches can be used to find this accurate description. Basically, there are three types are commonly used, i.e. modeling geometric parameters, modeling non-geometric parameters and model-free techniques. The first two methods are also called as model based techniques.

1) Modeling geometric parameters

A kinematics model is a mathematical description of the geometry and motion of a robot. A number of different approaches exist for developing the kinematics model of a robot manipulator. The most popular method of modeling robot kinematics is serially composing link models using the standard Denavit-Hartenberg (D-H) parameterization. The method based on homogeneous transformation matrices. These link models use only four geometric parameters per link to describe the relative displacement between coordinate frames of neighboring links. D-H modeling is relatively easy to use and often yields an algebraic inverse solution, which can be quickly computed. The procedure consists of establishing coordinate systems on each joint axis. Each coordinate system set of coefficients in the homogeneous transformation matrices.

However, the kinematic models do not have enough parameters to express any small variation in the actual robot structure away from the nominal. Small variations in the actual robot structure do not result in correspondingly small variations in model parameters. For example large changes in the model parameters occur when consecutive joints change from parallel to almost parallel planes. The result is instability in the numerical methods used during the identification phase. Also world and tool frames cannot be located arbitrarily and variations in robot geometry will therefore result in

variations in the position of these frames. However, D-H representation dominates the kinematics models used in most existing robot controllers. An excellent review of these different models, categorized into 4-, 5- and 6-link parameter models is given by Hollerbach [6].

2) Modeling non-geometric parameters

Non-geometric effects are usually modeled by adding extra terms to the overall geometric model of the manipulator. The analytical formulation of these terms is often inspired by prior experimental observations. Vincze [7] stated that non-geometric effects are mainly due to joint related characteristics and used a linear joint-dependent model for their correction. Alternative and more sophisticated joint-dependent formulations were also applied by Gong [8], Everett [9] and Meggiolara et al. [10].

3) Model-free techniques

Due to the complexity of the structure of many multi-DOF mechanisms, alternative modeling approaches proposed to approximate the error rather than modeling explicitly the different errors sources.

In the model-free approach, the relationship between the end-effector coordinates and the corresponding joint coordinates is fully or partly produced in a 'black-box' method. This means that the robot user does not have to formulate a priori any analytical model for correcting the errors in the robot pose. All the "intelligence" of finding an appropriate model is delegated to the approach itself. In fact, different well-established tools coming from the function approximation theory were used for this purpose, such as spline functions, polynomial functions, artificial neural networks and Genetic Programming (GP) [11, 12] and so on. The process does not need to start with a predefined model. It only needs to build up the calibration model from primitive model components during the calibration process. Since there is no iterative numerical parameter identification

involved, corresponding stability and conditioning issues are of no concern. It should be noted that very few papers in the literature make use of model-free techniques.

1.2.2.2 Pose Measurement

Measurement is the most difficult and time-consuming phase of robot calibration. The actual measured positions of the robot end-effector are compared with the positions predicted by the theoretic model to obtain the workspace inaccuracy data. Generally, six parameters are necessary to completely specify the position of a rigid body. The sufficiency requirements depend on the exact nature of the six conditions used to specify the position of the body. The measurement procedure must exhibit the individual parameters of the model in some way and the measurement system must be accurate enough to measure the affects of these parameters. A good model is useless without a measurement procedure and a system to match.

Different measurement methods and different measuring devices have been used so far for robot calibration tasks. The main differences are in the measurement method (contact or non-contact), the number of captured DOF (from 1 to 6), accuracy and costs [13]. Many Calibration of Robot Testing studies during the 1980's were done using a variety of measurement techniques ranging from expensive Coordinate Measurement (CMM) and Tracking Laser Interferometer Systems to ones that employed inexpensive customized fixtures. Some measurement devices are capable of measuring the full 6-demensional pose, some can measure only the 3D position and others, such as single theodolite, measure even less than that. Typical measurement devices for robot calibration are wire potentiometers [14], telescopic ball systems measured by radial distance transducers (LVDT) [15], interferometers [16, 17], ultrasonic systems [18], proximity sensors, imaging laser tracking systems [19, 20], single and stereo camera systems [21], magnetic trackers, theodolites [22, 23], cable driven systems, ball-bars and other systems traditionally used for machine-tool inspection [24].

Laser trackers are typically used in the automotive and aerospace industries for measuring and alignment of mechanical parts and assemblies. Figure 6 shows three manufactures of Laser Trackers [25].

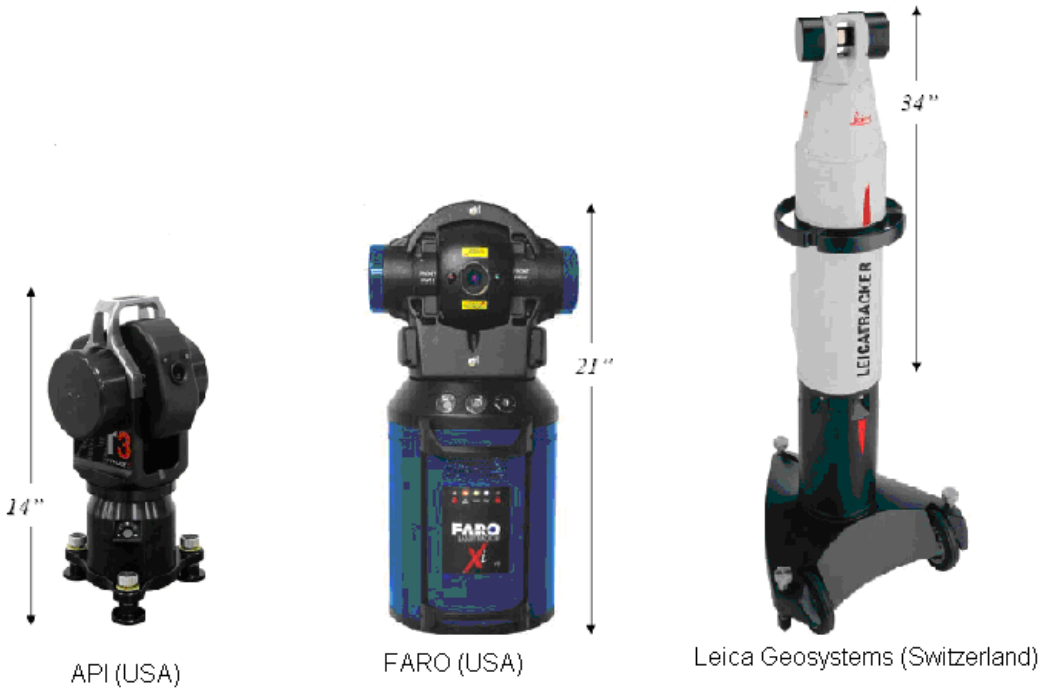

Figure 6. Three manufactures of Laser Trackers.

The FARO Laser Tracker X is a portable, contact measurement system that uses laser technology to accurately measure large parts and machinery across a wide range of industrial applications. It has a 70m (230-ft.) diameter range, achieves 0.025mm (0.001") 3-D single-point accuracy, and is rugged enough for the shop-floor environment. The system measures 3-D coordinates with its laser by following a mirrored spherical probe. High-accuracy, angular encoders — along with XtremeADM — Absolute Distance Measurement, reports the 3-D position of the probe in real-time.

Figure 7 shows the principle of Michelson interferometer [26]. One is looking "down" along the axis of two combined beams towards the light source. A beamsplitter mirror is used to bring the beams together from the two flat mirrors. It has a deliberately thin

reflective coating to permit about one-half of the light to pass through. If the light is of a single wavelength, fringes will form all along the optical axis of the combined beams, oriented perpendicular to this axis and will appear to stand still, even though the beams are traveling at the speed of light -- a standing wave phenomenon. To the eye, the fringes appear as alternating small rings of light and dark surrounding the central images of the light source.

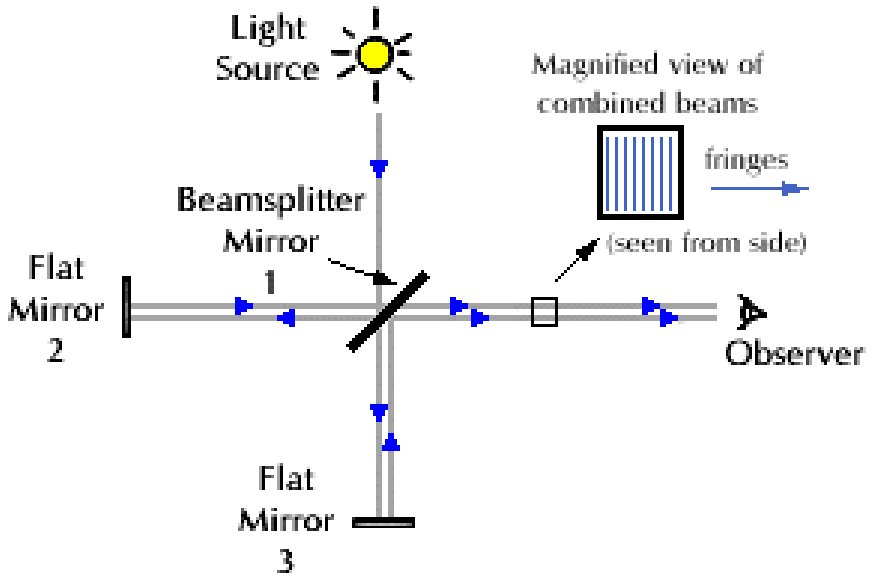

Figure 7. Michelson Interferometer

Another measurement system to describe here is the Krypton K600 solution. The main piece of the K series measurement system is the camera system, consisting in three linear CCD cameras, shown in figure 8. The camera system relies on infra red light active LEDs, and therefore they cannot be seen by the human eye. When a LED is picked by the three linear cameras the computer calculates its exact position in the 3D space.

Figure 8. Krypton K600 Camera system (Courtesy of Metris).

The illustration of the measurement steps of the K600 is shown in Figure 9. The calculation is achieved by comparing the image of the 3 linear CCD cameras, from the effect of having 3 planes intersecting on the LED position, which is then calculated relative the pre-calibrated camera. According to the manufacturer the system is capable of tracking up to 256 LEDs simultaneously, through computer controlled strobing. This simultaneous multiple point tracking allows the measurement of the position and orientation of objects by attaching to them 3 or more LEDs and measuring their positions simultaneously. The system has a single point accuracy starting at 60 μ and is capable of measuring targets at 6 m distance from the camera.

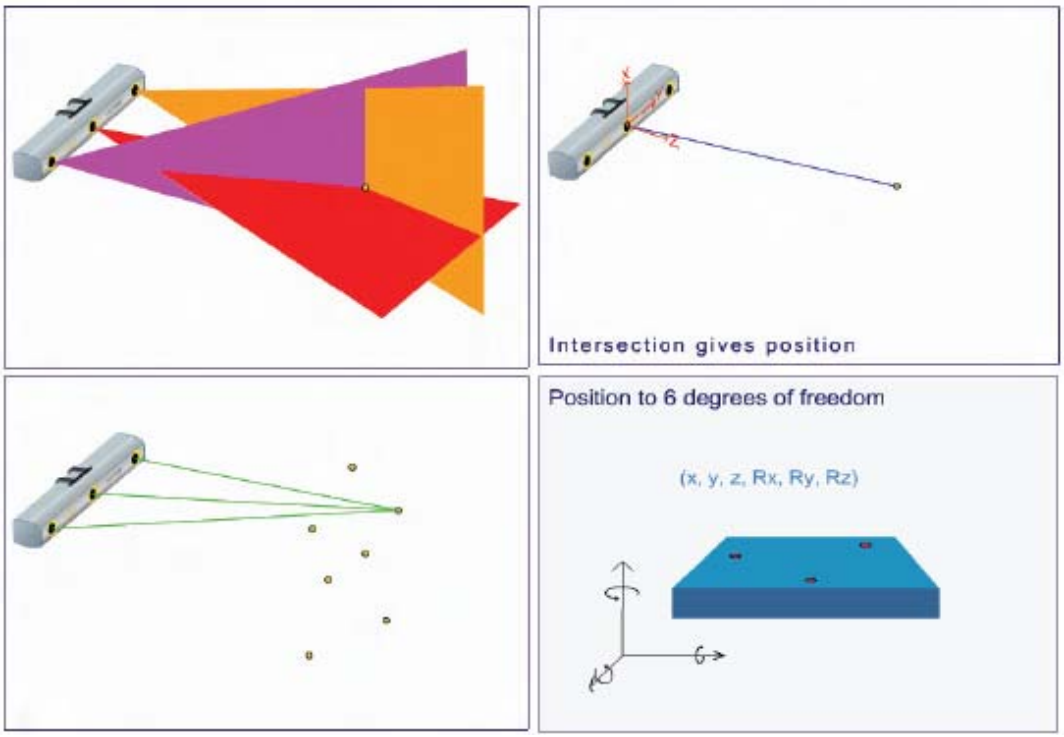

Figure 9. Illustration of the measurement steps of the K600 (Courtesy of Metris).

This measurement system is a fundamental piece of metrology, which can be used for robot calibration and other application like motion analysis and 3D CMM inspection. This system is then valid for any calibration procedure that relies on measuring the pose of the end-effector of the manipulator. All is needed is fixing the LEDs precisely on the end-effector and start the measurement, which takes only minutes.

Figure 10 and figure 11 illustrate a ball bar measurement system. The Ball Bar is used to quickly and accurately check system accuracy. Renishaw's QC10 ballbar is a linear displacement sensor based tool that provides a simple, rapid check of a CNC machine tool's positioning performance to recognized internationals standards [27]. The Renishaw QC10 ballbar system consists of a calibrated sensor within a telescopic ball-ended bar, plus a unique mounting and centration system. It is not to be confused with the fixed length ballbars used for CMM (coordinate measuring machine) calibration. A QC10 ballbar test involves asking the machine to scribe a circular arc or circle. Small

deviations in the radius of this movement are measured by a transducer in the ballbar and captured by the software.

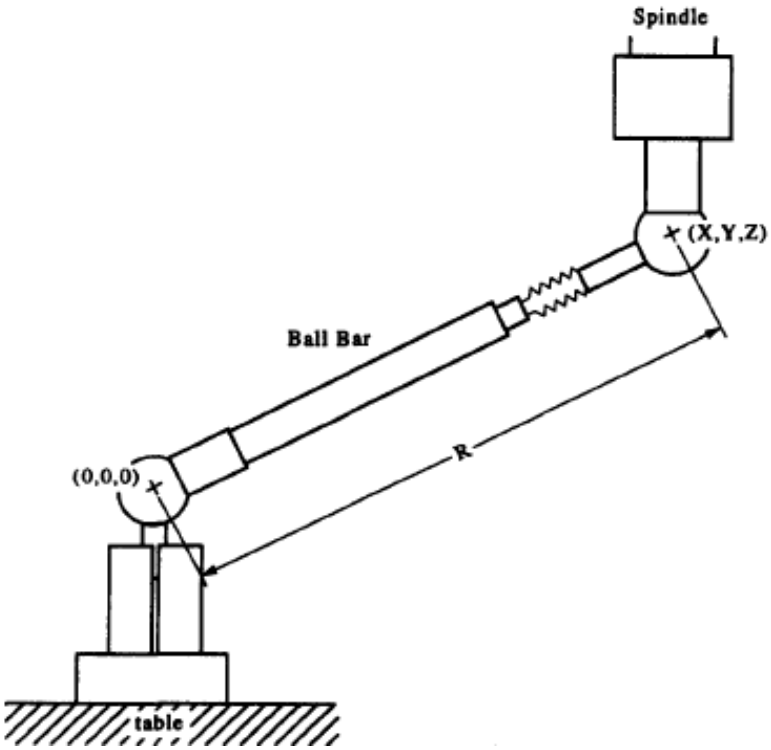

Figure 10. Error measurement using the kinematic ball bar.

Figure 11. QC10 ballbar system (courtesy of Renishaw)

1.2.2.3 Kinematics Identification

Parameter identification involves numerical methods. In this phase, kinematic parameter errors are identified, by minimizing the collected workspace inaccuracy in the least mean square sense. A major contribution to the Kinematics Identification phase of Robot Calibration was the paper by Chi-Haur Wu [28], in which the Identification Jacobian, a matrix relating end-effector pose errors to robot kinematics parameters errors, is systematically derived. This mathematical tool is very useful for both machine accuracy analysis and machine calibration. Another contribution by Wu and his co-authors was the paper [29] that introduced two techniques for accuracy compensation.

Recently, researchers have addressed some theoretical issues to improve kinematic identification strength and efficiency. Such issues include: the condition number of the identification Jacobian by Khalil et al [30], the optimum calibration configurations determination by Born and Meng [31]. David Daney [32] use algebraic methods for parameter identifications, which can be an alternative of the commonly used least-squares method.

1.2.2.4 Kinematics Compensation

This is the final and decisive step in robot kinematic calibration, which is the implementation of the new model in the position control software of the robot. Sometimes is referred to as the correction step. Due to the difficulty in modifying the kinematic parameters in the robot controller directly, joint compensations are made to of the robot obtained by solving the inverse kinematics of the calibrated robot.

Since the inverse kinematics of the calibrated robot, generally not solvable analytically, numerical algorithms such as the Newton-Raphson approach are usually applied to solve the model to find the joint corrections needed to compensate for Cartesian errors. With

the Newton-Raphson algorithm, on- line compensation is problem due to the computation expense and the algorithm breaks down in the vicinity of robot singular configurations, because the approach is based on the iterative inversion of the compensation Jacobian. Veitschegger and Wu [29] presented the differential transformation compensation method in which two nominal inverse problems are solved for one task point compensation.

1.3 Scope of this research

There are many error sources may cause a robot to deviate from its ideal kinematics model. Temperature variation of the environment, servo motor errors, structural deflections, imperfect gears, gear and bearing runout, backlash, and machining tolerances all lead to the inaccuracies which appear in the robot model. This thesis will concentrated on modeling structural deformations, finding the exact kinematics parameters to predict the errors from all the remaining sources of inaccuracies not specifically modeled. For clarity, the scope of the thesis is summarized as follows:

- Kinematics modeling of serial and parallel robot, including the inverse and forward kinematics of the studied robot.
- Error modeling of serial and parallel robot separately.
- Error modeling of the proposed hybrid redundant robot
- Numeric simulation and analysis of the error model

1.4 Strategy used for this work

The robot under study is a redundant hybrid manipulator which consists of two relatively independent sub-structures, the first part is the parallel mechanism driven by six water hydraulic cylinders which contributes the full six degrees of freedom for the end-effector. The second part is the carriage which made of serial links offers additional four degrees of freedom for Hexa-WH. These four degrees of freedom can provide two translational

motions and two rotational motions for enlarging the workspace and offering the robot higher mobility.

Based on the specific structure of the proposed robot, the general strategy of this work is divided into two parts. Both serial link and parallel one will be illustrated separately then combine them together to develop a final hybrid solution. For the kinematics modeling of the proposed robot, the D-H convention will be used for serial link, and vector algorithm method will be used for parallel mechanism. For the error modeling of the robot, the vector differential method will be utilized to derive the serial link, parallel mechanism and the whole robot solution.

1.5 Structure of this study

The structure of this study is as follows:

- Section 1 serves as introduction. The main objective of this part is to introduce the background and scope of this paper, and the literatures are also reviewed.
- Section 2 reviews the error analysis methods used for serial robot and parallel robot respectively. In this part, the general structure and classification of robots are also illustrated.
- Section 3 specified the robot under study, and vector differential method is used to derive the error model.
- Computer simulation results and analysis are presented in section 4.
- Section 5 gives conclusions and outlook of the work.

2 ERROR ANALYSIS METHODS USED FOR SERIAL ROBOT AND PARALLEL ROBOT

In this section, the general structure and classification of robots will be presented first. Then the commonly used error analysis methods for serial robots and parallel manipulators are discussed respectively.

2.1 Classification of robots

Robots can be classified according to various criteria, such as their degrees of freedom, kinematics structure, drive technology, workspace geometry, and motion characteristics [33]. What follows will discuss these classifications in turn.

2.1.1 Classification by degrees of freedom

In general, to operate an object freely in three-dimensional space, a manipulator should possess 6 degrees of freedom. From this point of view, we call a manipulator which has more than 6 degrees of freedom as a *redundant robot*, and if the degrees of freedom are less than 6 we call it as a *deficient robot*.

2.1.2 Classification by kinematics structure

Manipulator can also be classified according to their structural topologies. A robot is said to be a *serial robot* or *open-loop manipulator* if its kinematics structure takes the form of an open-loop chain, a *parallel manipulator* if it consists of a closed-loop chain, and a *hybrid manipulator* if it is made of both open- and closed-loop chains.

2.1.3 Classification by drive technology

There are three popular drive technologies are used to manipulators, i.e. *electric*, *hydraulic*, and *pneumatic*. Most manipulators use either electric DC servomotors or stepper motors, because they are clean and relatively easy to control. However, when high-speed and/or high-load-carrying capabilities are needed, hydraulic or pneumatic drive is preferred. A major disadvantage associated with the use of a hydraulic drive is the possibility of leaking oils. Additionally, a hydraulic drive is inherently flexible, due to the bulk modulus of oil. Although a pneumatic drive is clean and fast, it is difficult to control because air is a compressible fluid.

2.1.4 Classification by workspace geometry

The workspace of a manipulator is defined as the volume of space the end-effector can reach. According to the workspace of a manipulator, a robot can be classified as follows:

Cartesian robot: Perhaps the simplest kinematic structure of robot arm is made up of three mutually perpendicular prismatic joints. This type of robot is known as a Cartesian robot, which is used for pick and place work, application of sealant, assembly operations, handling machine tools and arc welding. Obviously, the regional workspace of a Cartesian robot is a rectangular box. Figure 12 shows a Cartesian robot set up in Lappeenranta University of Technology (LUT).

Figure 12. 3-Axis Cartesian robot in LUT

Cylindrical robot: A robot arm is called a cylindrical robot if either the first or second joint of a Cartesian robot is replaced by a revolute joint. The schematic of cylindrical robot is shown in Figure 13.

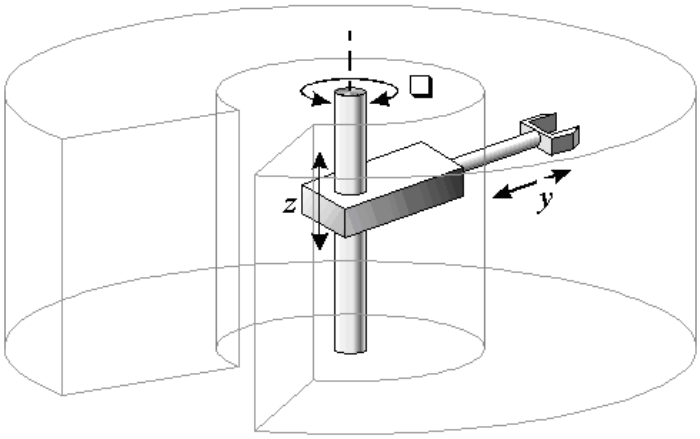

Figure 13. The Schematic of cylindrical workspace

Cylindrical robot is used for assembly operations, handling at machine tools, spot welding, and handling at die-casting machines. It's a robot whose axes form a cylindrical coordinate system [34]. Figure 14 shows a prototype of cylindrical robot.

Figure 14. Robot RT33 (SEIKO Instruments) with cylindrical workspace

Spherical/Polar robot: A robot arm is called a spherical robot if the first two joints are made up of two intersecting revolute joints and the third is a prismatic joint. The schematic of spherical robot is shown in Figure 14.

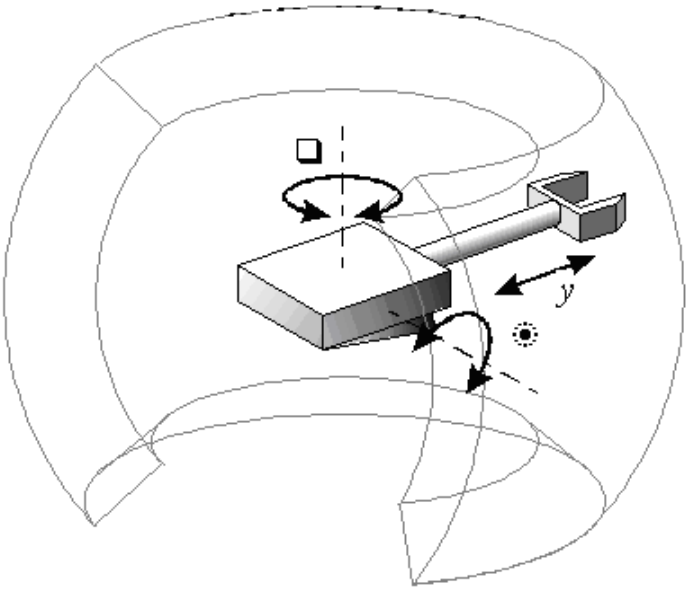

Figure 15. The Schematic of spherical/polar workspace

Spherical/Polar robot is used for handling at machine tools, spot welding, and die-casting, fettling machines, gas welding and arc welding. It's a robot whose axes form a polar coordinate system.

Articulated robot: A robot is said to be an articulated robot if all three joints are revolute. The workspace of an articulated robot is very complex, typically a crescent shaped cross section. Many industrial robots are of the articulated type. KUKA industrial robot is an articulated robot, as is shown in Figure 16 and Figure 17.

Figure 16. 6-axis articulated robot (KUKA industrial robot)

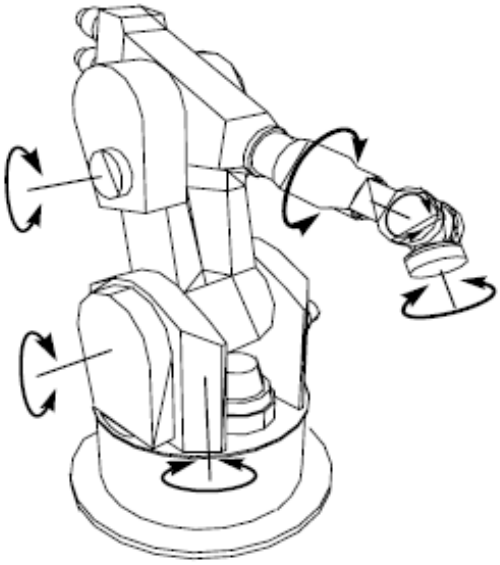

Figure 17. A KUKA-160 industrial robot)

Articulated robot is used for assembly operations, die-casting, fettling machines, gas welding, arc welding and spray painting. It's a robot whose arm has at least three rotary joints.

SCARA robot: It consists of two revolute joints followed by a prismatic joint. In addition, all three joint axes are parallel to each other and usually point along the direction of gravity. Thus the first two actuators do not have to work against the gravitational forces of the links and the payload. Which are used for pick-and-place work, application of sealant, assembly operations and handling machine tools. The schematic of spherical robot is shown in Figure 18.

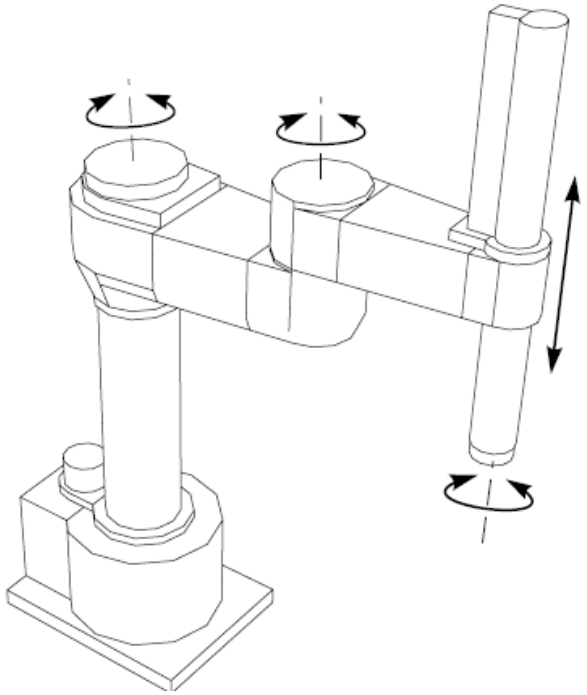

Figure 18. The Schematic of SCARA robot

Parallel robot: is a device for performing manipulations, where the end-effector is connected to the base via multiple kinematic chains. Any two chains thus form a closed loop. It's a robot whose arms have concurrent prismatic or rotary joints. Figure 19 shows a horse simulator with Stewart- Gough mechanism built in LUT.

Figure 19. A horse simulator with Stewart- Gough mechanism developed in LUT

Figure 20 shows another 5-DOF hydraulic parallel robot developed in LUT, which is the first version of IWR and can be used for machining and welding.

Figure 20. Penta-WH : The first prototype of IWR version developed in LUT

2.1.5 Classification by motion characteristics

Robot manipulators can also be classified according to their nature of motion. A rigid body is said to perform a planar motion if all particles in the body describe plane curves that lie in parallel planes. A mechanism is said to be a planar mechanism if all the moving links in the mechanism perform planar motions that are parallel to on another. A manipulator is called a planar manipulator if its mechanism is a planar mechanism. Figure 21 shows a 3-DOF planar parallel manipulator.

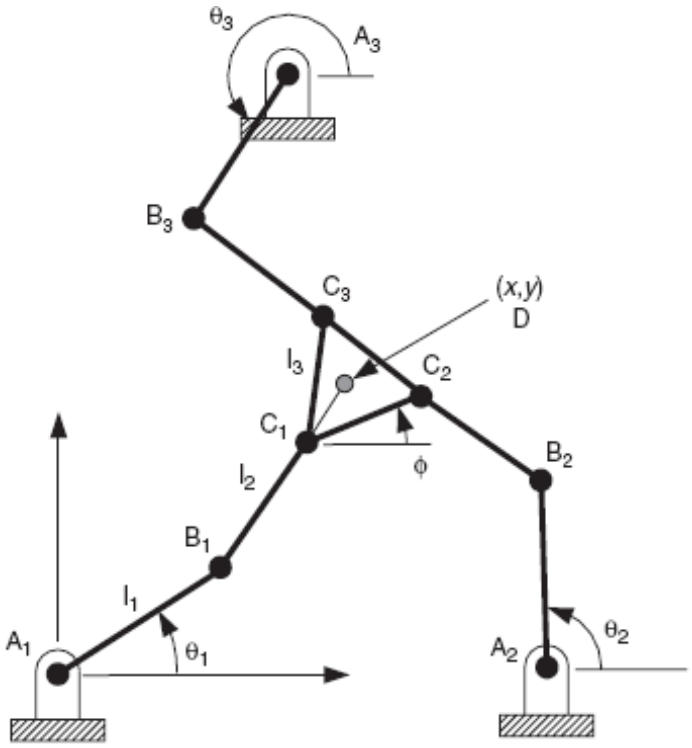

Figure 21. A schematic of the planar 3RRR manipulator

A rigid body is said to be under a spherical motion if all particles in the body describe curves that lie on concentric spheres. Thus when a rigid body performs a spherical motion, there exists at least one stationary point. A mechanism is said to be a spherical mechanism if all the moving links perform spherical motions about a common stationary

point. A manipulator is called a spherical manipulator if it is made up of a spherical mechanism. Figure 22 shows a 3-dof spherical parallel manipulator. In this mechanism, all the revolute joints intersect at a common center point O. The Agile Eye is a 3-DOF 3-RRR spherical parallel manipulator developed for the rapid orientation of a camera. Its mechanical architecture leads to high velocities and accelerations. A spherical manipulator can also be used as a pointing device.

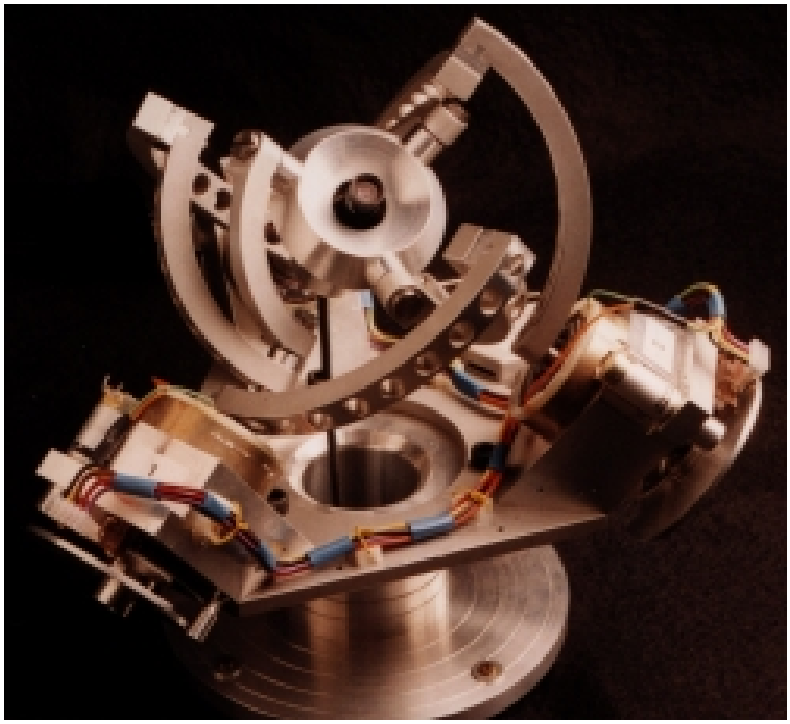

Figure 22. 3-DOF spherical parallel manipulator: Agil Eye (Courtesy of Laval University Robotics Laboratory)

A rigid body is said to perform a spatial motion if its motion cannot be characterized as planar or spherical motion. A manipulator is called a spatial manipulator if at least one of the moving links in the mechanism possesses a general spatial motion.

2.2 The methods of error analysis used for serial robot

A serial manipulator consists of several links connected in series by various types of joints, typically revolute and prismatic joints. One end of the manipulator is attached to the ground and the other end is fee to move in space. For this reason a serial manipulator is sometimes called an open-loop manipulator.

An overview of robot calibration techniques and the identification of three calibration levels are introduced and discussed in [35]. Level 1 is the joint level calibration, level 2 is the entire robot kinematic model calibration, and level 3 is the non-kinematic (non-geometric) calibration.

In order to obtain appropriate parameter values, the international standard ISO 9283 was published in 1998 for evaluating different performance criteria for industrial robot [36]. The most important criteria, and also the most commonly used, are accuracy of pose (AP) and repeatability of pose (RP). Repeatability is a measure of the ability of the robot to move back to the same position and orientation over and over again. It is particularly important when the robot is moved towards the command positions manually ("Teach-In"). Accuracy is defined as the ability of the robot to precisely move to a desired position in 3-D space. If the robot program is generated by a 3D simulation ("off-line programming"), absolute accuracy is vital, too. Both are generally influenced in a negative way by kinematics factors. Here especially the joint offsets and deviations in lengths and angles between the individual robot links take effect. These concepts can be shown graphically in figure 23.

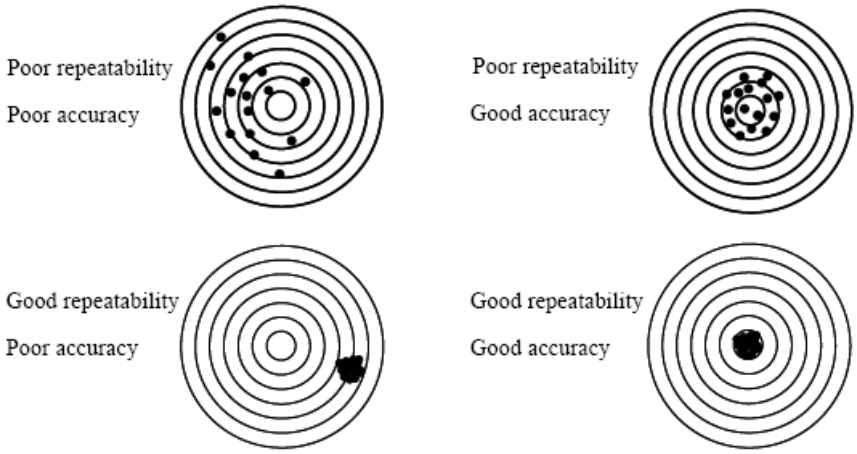

Figure 23. Repeatability and accuracy of a shooter evaluated from the observation of different shooting targets.

For the error modeling of serial robot, the most commonly used method of representing the relationship between two consecutive link coordinate frames is the homogeneous transformation matrix defined by Denavit and Hartenberg [37]. Their representation uses four kinematics parameters to completely describe this relationship. Geometric errors in the manipulator's structure will produce corresponding errors in these kinematics parameters. The kinematics errors in the manipulator structure for modeling geometric errors can be divided into two categories:

1) Errors in the joint variables,
2) Errors in the fixed kinematics parameters.

The schematic diagram of D-H convention is shown in Figure 24. The procedure consists of assigning a coordinate system to each link at the joint axis and then expressing the relationship between consecutive coordinate systems with homogeneous transformation matrices. All of the individual link transformation matrices may then be multiplied together to produce one transformation relating the coordinate system in the end-effector to the base coordinate frame.

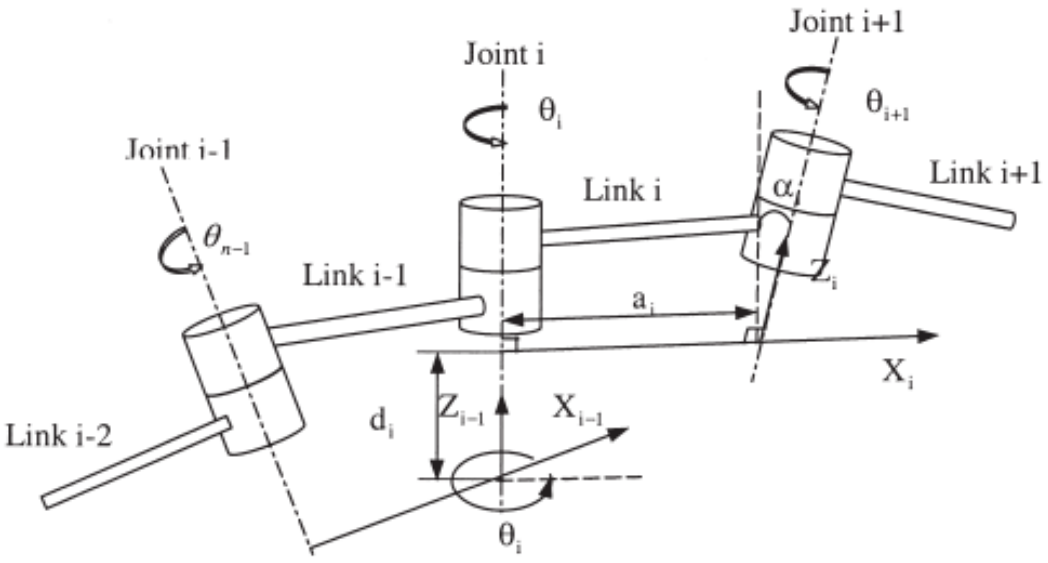

Figure 24. Graphical representation of D-H parameters [37]

The relative translation and rotation between $i-1th$ and ith coordinate systems are given by the four parameters homogenous transformation matrix ${}^{i-1}A_i$ as shown in (1).

$$ {}^{i-1}A_i = \begin{bmatrix} c\theta_i & -c\alpha_i s\theta_i & s\alpha_i s\theta_i & a_i c\theta_i \\ s\theta_i & c\alpha_i c\theta_i & -s\alpha_i c\theta_i & a_i s\theta_i \\ 0 & s\alpha_i & c\alpha_i & d_i \\ 0 & 0 & 0 & 1 \end{bmatrix} \tag{1} $$

where $c\theta_i$ denotes $\cos\theta_i$, and $s\theta_i$ denotes $\sin\theta_i$.

As pointed out by Hayati [38], small errors in the end-effector position could not be modeled by small errors in the D-H link parameters in the case of two consecutive parallel joints or nearly parallel joints. This causes numeric instability during the identification process. In order to avoid the singularity problem, a small rotation of β about the y-axis, Rot (y, β), is introduced into the homogeneous transformation. This work was later expanded by Veitschegger and Wu [29], to include second order terms.

P.S. Shiakolas et al [39] discussed industrial robot characteristics of accuracy and repeatability by using D-H parameters.

The definition of the modified five D-H parameters is shown in Figure 25.

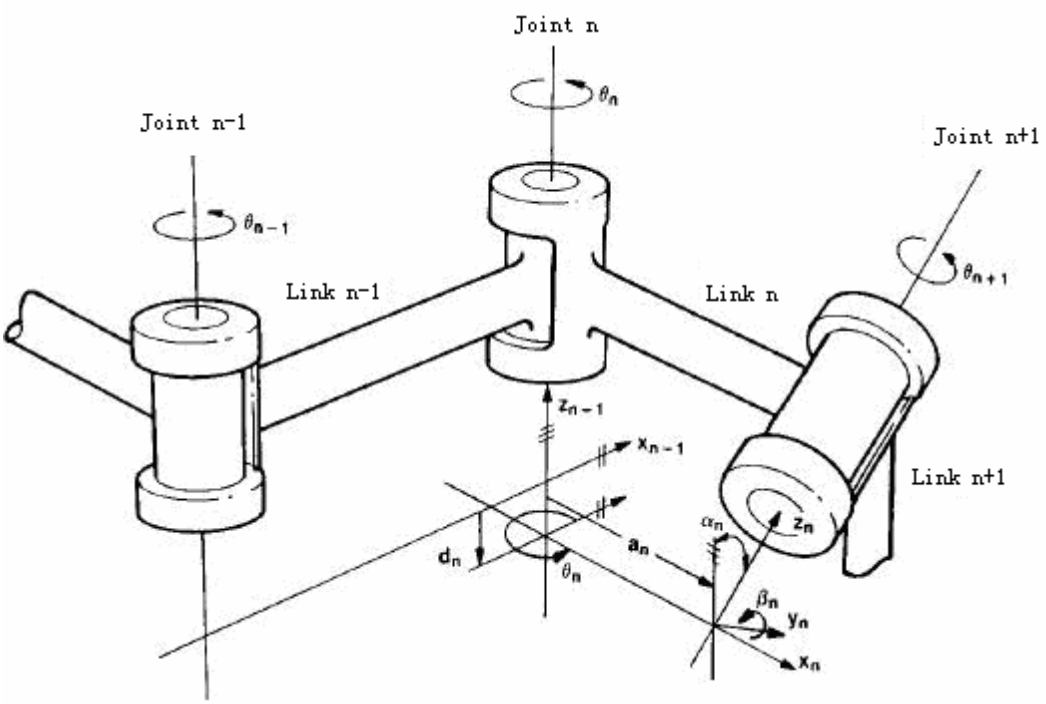

Figure 25. Definitions of parameters for modified D-H link

The relative translation and rotation between $i-1th$ and ith coordinate systems are given by the homogenous transformation matrix ${}^{i-1}A_i$ as shown in (2).

$$ {}^{i-1}A_i = \begin{bmatrix} c\theta_i c\beta_i - s\theta_i s\alpha_i s\beta_i & -s\theta_i c\alpha_i & c\theta_i s\beta_i + s\theta_i s\alpha_i c\beta_i & a_i c\theta_i \\ s\theta_i c\beta_i + c\theta_i s\alpha_i s\beta_i & c\theta_i c\alpha_i & s\theta_i s\beta_i - c\theta_i s\alpha_i c\beta_i & a_i s\theta_i \\ -c\alpha_i s\beta_i & s\alpha_i & c\alpha_i c\beta_i & d_i \\ 0 & 0 & 0 & 1 \end{bmatrix} \qquad (2) $$

where c denotes cosine and s denotes sine respectively.

Another method used for industrial robot calibration is so-called “S-model” developed by Stone, Sanderson, and Neuman [40]. The S-Model is a mathematical model which can be used to describe the exact kinematic structure of any robotic manipulator with rigid links. In contrast to the D-H model, the S-Model is directly applicable to identification. “S-model” using six parameters per link and then convert these parameters to the D-H parameters. They perform calibration of the manipulator by measuring the Cartesian positions of a point attached consecutively to each of the links while rotating the link through its range. Figure 26 shows the definitions of S-Model kinematic parameters.

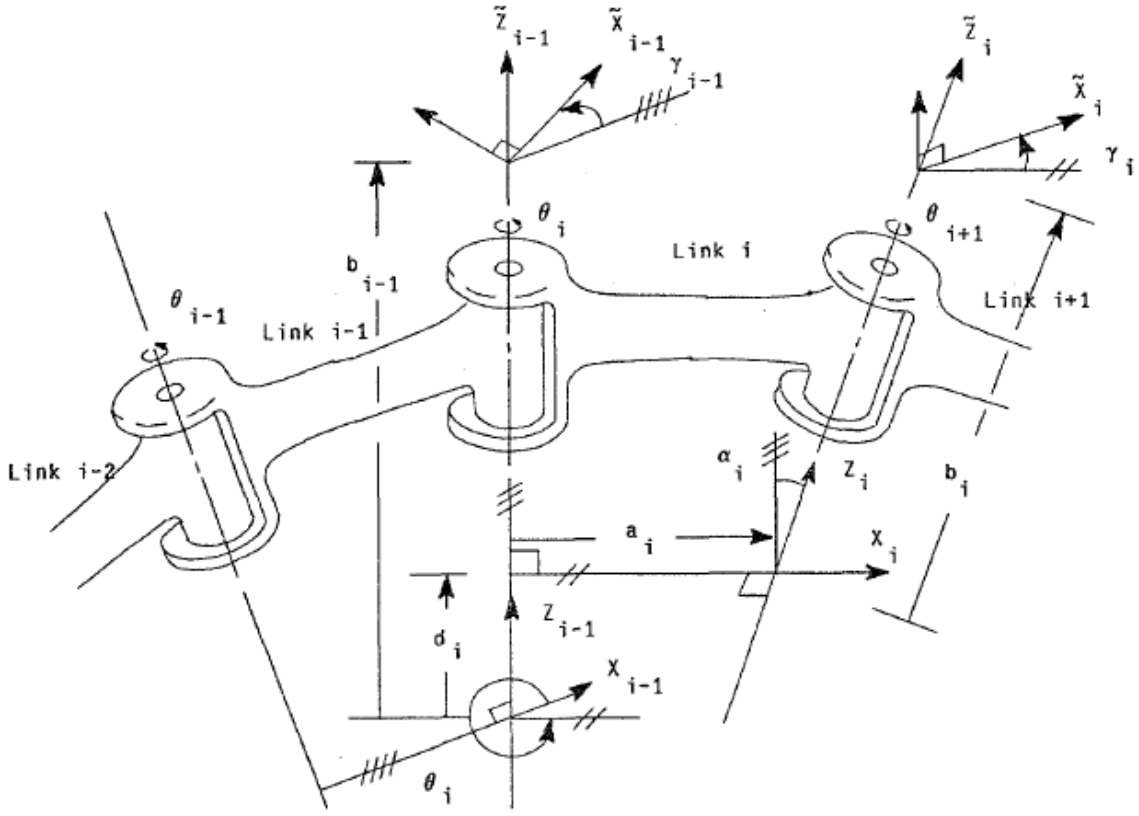

Figure 26. Definitions of S-Model Kinematic parameters

The relationship between the four D-H parameters and the six S-Model parameters can be written as follows:

$$\theta_i = \beta_i + \gamma_{i-1} \tag{3}$$

$$d_i = \bar{d}_i + b_{i-1} \tag{4}$$

$$a_i = \bar{a}_i \tag{5}$$

$$\alpha_i = \bar{\alpha}_i \tag{6}$$

2.3 The methods of error analysis used for parallel robot

Over the past decades, more and more attentions have been given to parallel robots. A parallel robot is a closed-loop mechanism in which the mobile platform is connected to the base by at least 2 serial kinematic chains (legs). Parallel mechanisms present themselves as feasible alternatives to their serial counterparts in situations where the demand for high speed, accurate motion and dynamic loading outweighs those for workspace and dexterity.

Nowadays, parallel robots are more and more involved in new applications within domains such as high speed machining, pick and place or medical. However, improving the accuracy of these machines is still a challenge and intensive research work. It has been recognized that the pose error of a parallel robot with six degrees of freedom can in principle be fully compensated by software. Over the past decade, a number of approaches for dealing with the calibration of the 6-DOF parallel mechanism systems have been developed and reported. In this section, we will adopt the classification originally proposed by Hollerbach in [13], According to this author, calibration methods usually fall into one of the following categories:

- Open-loop methods;
- Closed-loop methods;
- Implicit-loop methods;
- Screw-axis methods;

- Self-calibration methods.

Notice that the distinction between some of the methods is often small and arbitrary. For example, a given open-loop method may constrain some degrees of freedom, and also measure others, thus mixing open and closed-loop methods. In addition, parallel structures have a mixture of sensed and un-sensed joints, the latter being formally not different from the task kinematics of passive joints for closed-loop methods.

2.3.1 Open-loop methods

The most common and widely used calibration method is the open-loop method, in which a manipulator is placed in a number of poses and the complete or partial end-effector pose is measured. The term "open-loop" refers in fact to an end-point that is positioned freely in space. In general, this method tends to be used for the calibration of serial mechanisms rather than parallel ones. Examples of these are:

- Ota et al. [24], Takeda et al [41] performed calibration of parallel robot by using a Double Ball Bar system.
- The work of Koseki [42] considering the calibration of a 6-legged parallel arm by means of a laser tracking coordinate-measuring system;
- The work of Besnard and Khalil [23] in which a Stewart platform is calibrated with the help of two inclinometers;
- The calibration of a Stewart platform using pose measurements obtained by a single theodolite by Zhuang [22].

2.3.2 Closed-loop methods

As opposed to the classical open-loop method, the closed-loop method does not require an external measurement system. For serial mechanisms, calibration is achieved by sensing joint angles only, by attaching the end-effector to the environment in order to

form a mobile closed kinematic chain. This approach was based on a constrained optimization technique involving a large number of redundant parameters, the constrained equations arising from the fact that the closed-loop had to remain closed for all the configurations. Finally, extensions of the closed-loop method to multiple closed-loop systems have been considered in [43, 44].

2.3.3 Implicit-loop methods

In an implicit-loop method, the error enters the kinematic loop equation implicitly, rather than being the explicit output of a conventional input – output formulation. The main advantage is that difficult-to-model error sources, such as input noise and backlash, can be included in the merit function to be optimized. Wampler and Hollerbach [45] used the implicit-loop method in order to demonstrate a unified formulation on the self-calibration of both serial and parallel robots. Their paper included an application to two 6-DOF mechanisms.

2.3.4 Screw-axis methods

The basic principle of screw-axis methods is slightly different from that of kinematic-loop methods. In fact, each axis is now identified independently as a screw. The major advantage lies in the fact that kinematic parameters can be identified without the need for solving a non-linear optimization problem. The most commonly known variant is called Circle Point Analysis (CPA). It consists of measuring the end-point position by acting on a different joint at a time. It can then be regarded as an open-loop method with this particular pose selection. Examples of the application of the CPA technique can be found in [46].

2.3.5 Self-calibration methods

Self calibration methods using extra sensors on the passive joints have been also proposed for parallel robots. Self-calibration is similar to the closed-loop method, except that additional sensor data is often used to facilitate the calibration; hence, it may be viewed as a variant of the closed-loop method. This method has the potential for removing the dependence on any external pose-sensing information and has the capability of producing accurate measurement data over the entire workspace of the system with a fast measuring rate. Moreover, it is completely non-invasive. Probably for these reasons, self-calibration methods are gaining popularity among researchers working with the calibration of parallel robots, as can be seen by the number of papers based on this particular method.

1) In the method of Zhuang and Liu [47], a limited number of passive Universal joints are needed to be measured.
2) Gael Ecorchard and Patrick [48] Maurine proposed a new geometrical self-calibration method for Delta parallel robots with compensation of the non-geometrical gravity effects.
3) Wisama Khalil and Sebastien Besnard [49] presented a new method for self-calibration of Stewart-Gough parallel without extra sensors. The calibration makes use of the motorized prismatic joint positions corresponding to some sets of configurations where in each set either a passive Universal joint or a passive spherical joint is fixed using a lock mechanism.

The calibration methods based on redundant sensors on the passive joints adjust the values of the kinematic parameters in order to minimize a residual between the measured and the calculated values of the angles of these joints. In order to get appropriate accuracy for the identified parameters, big accuracy is needed on these sensors. Putting sensors on an already manufactured robot is not a trivial problem; it must be foreseen while designing the robot. It is to be noted that redundant sensors on the U-joints have been proposed also to get an analytical solution of the direct kinematic model [50, 51]. But in this case moderate accuracy is sufficient.

Moreover, the calibration methods also can be classified into three main types according to J.P. Merlet [52]:

- *External calibration:* methods based on total or partial measurements of the platform poses or of other geometrical elements of the robot through an external device.
- *Constrained calibration:* methods that rely on a devoted mechanical system that constrains the robot motion during the calibration process.
- *Auto-calibration or self-calibration:* methods that rely on the measurements of the internal sensors of the robots. In that case it is required that a N DOF robot has m>N internal sensors.

3 KINEMATIC MODELLING AND ANALYSES OF IWR

In this section, the structure of the proposed robot will be illustrated first, and then the forward and inverse kinematics of the robot is to be derived.

3.1 Structure of IWR

The kinematics of the proposed hybrid robot as shown in Fig.1 can be divided into two parts, the serial part and the parallel one, i.e., the carriage and Hexapod. To simplify its analysis, the two parts will be first carried out respectively, and then combined them together to obtain the final solutions.

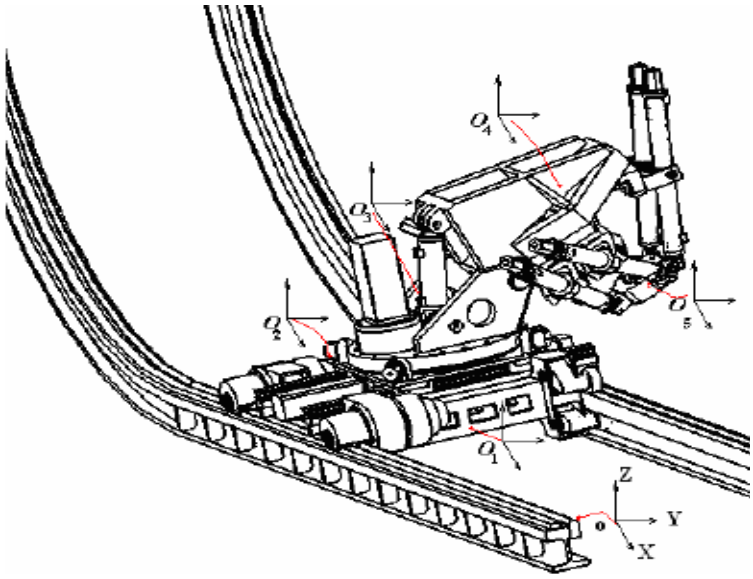

Figure 27. 3D model of IWR

3.2 Kinematic analysis

Generally, the kinematics analysis of a robot is divided into two types, i.e. forward kinematics (FK) and inverse kinematics (IK). FK is computation of the position and orientation of robot's end-effector as a function of its joint angles, and IK is the process of determining the parameters of a jointed flexible object (a kinematic chain) in order to achieve a desired pose (position and orientation). In a kinematic analysis the position, velocity and acceleration of all the links are calculated without considering the forces that cause this motion. The relationship between motion, and the associated forces and torques is studied in robot dynamics. In this paper, we only consider the position kinematics of the studied robot.

The forward position kinematics (FPK) solves the following problem: "Given the joint positions, what is the corresponding end effector's pose?"[53]

For serial chains: the solution is always unique, one given joint position vector always corresponds to only one single end-effector pose. The FK problem is not difficult to

solve, even for a completely arbitrary kinematic structure. Methods used for a forward kinematic analysis:

- using straightforward geometry
- using transformation matrices

For parallel chains (Stewart Gough Manipulators): the solution is not unique, one set of joint coordinates has more different end-effector poses. In case of a Stewart Platform there are 40 poses possible which can be real for some design examples. Computation is intensive but solved in closed form with the help of algebraic geometry.

3.3.1 Forward kinematics of the studied robot

1) For the carriage

Based on the convention of Denavit-Hartenberg coordinate system, the principle of the 4-DOF carriage mechanism is established in Figure 28, which provides four degrees of freedom at the end-effector, including two translational movements and two rotational movements.

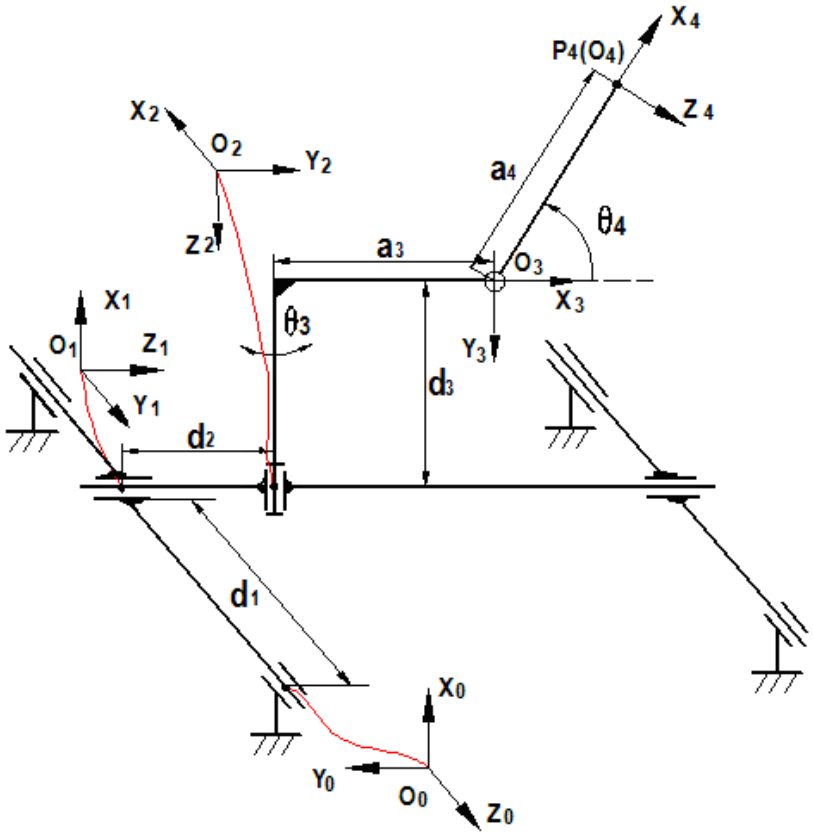

Figure 28. Coordinate system of carriage

Using the coordinate systems established in Figure 28, the corresponding link parameters are given in Table1. Substituting the D-H link parameters into (1), we can obtain the D-H homogeneous transformation matrices ${}^{0}\mathbf{A}_{1}$, ${}^{1}\mathbf{A}_{2}$, ${}^{2}\mathbf{A}_{3}$ and ${}^{3}\mathbf{A}_{4}$.

Table1. D-H Parameters of carriage

Joint i	α_i	a_i	d_i	θ_i
1	$\pi/2$	0	d_1(var)	0
2	$\pi/2$	0	d_2(var)	$\pi/2$
3	$\pi/2$	a_3	d_3	θ_3(var)
4	$-\pi/2$	a_4	0	θ_4(var)

$$ {}^{0}\mathbf{A}_{1} = \begin{bmatrix} 1 & 0 & 0 & 0 \\ 0 & 0 & -1 & 0 \\ 0 & 1 & 0 & d_1 \\ 0 & 0 & 0 & 1 \end{bmatrix} \tag{7} $$

$$ {}^{1}\mathbf{A}_{2} = \begin{bmatrix} 0 & 0 & 1 & 0 \\ 1 & 0 & 0 & 0 \\ 0 & 1 & 0 & d_2 \\ 0 & 0 & 0 & 1 \end{bmatrix} \tag{8} $$

$$ {}^{2}\mathbf{A}_{3} = \begin{bmatrix} c\theta_3 & 0 & s\theta_3 & a_3 c\theta_3 \\ s\theta_3 & 0 & -c\theta_3 & a_3 s\theta_3 \\ 0 & 1 & 0 & d_3 \\ 0 & 0 & 0 & 1 \end{bmatrix} \tag{9} $$

$$ {}^{3}\mathbf{A}_{4} = \begin{bmatrix} c\theta_4 & 0 & -s\theta_4 & a_4 c\theta_4 \\ s\theta_4 & 0 & c\theta_4 & a_4 s\theta_4 \\ 0 & -1 & 0 & 0 \\ 0 & 0 & 0 & 1 \end{bmatrix} \tag{10} $$

Then the resulting homogeneous transformation matrix can be obtained by multiplying the matrices of ${}^{0}\mathbf{A}_{1}$, ${}^{1}\mathbf{A}_{2}$, ${}^{2}\mathbf{A}_{3}$ and ${}^{3}\mathbf{A}_{4}$.

$$ {}^{0}\mathbf{A}_{4} = {}^{0}\mathbf{A}_{1}\,{}^{1}\mathbf{A}_{2}\,{}^{2}\mathbf{A}_{3}\,{}^{3}\mathbf{A}_{4} = \begin{bmatrix} s\theta_4 & 0 & c\theta_4 & d_3 + a_4 s\theta_4 \\ -s\theta_3 c\theta_4 & -c\theta_3 & s\theta_3 s\theta_4 & -d_2 - a_3 s\theta_3 - a_4 s\theta_3 c\theta_4 \\ c\theta_3 c\theta_4 & -s\theta_3 & -c\theta_3 s\theta_4 & d_1 + a_3 c\theta_3 + a_4 c\theta_3 c\theta_4 \\ 0 & 0 & 0 & 1 \end{bmatrix} \tag{11} $$

Based on (11), the forward kinematics can be written as follows

$$ p_x = d_3 + a_4 s\theta_4 \tag{12} $$

$$ p_y = -d_2 - a_3 s\theta_3 - a_4 s\theta_3 c\theta_4 \tag{13} $$

$$ p_z = d_1 + a_3 c\theta_3 + a_4 c\theta_3 c\theta_4 \tag{14} $$

2) For the Hexa-WH

Figure 29 shows a schematic diagram of hexa-WH parallel mechanism, for the purpose of analysis, two Cartesian coordinate systems, frames $O_4(X_4, Y_4, Z_4)$ and $O_5(X_5, Y_5, Z_5)$ are attached to the base plate and the end-effector, respectively. Six variable limbs are connected with the base plate by Universal joints and the task platform by Spherical joints.

For the forward kinematics (FK) problem, the limb lengths l_i are given, and the position and orientation vector of the end-effector are to be found. The position vector contains three scalar unknowns, while the rotation matrix contains nine scalar unknowns. The FK is a more complex problem than its dual inverse kinematics (IK) counterpart for serial robot. FK is an area where a lot of progress has been made thanks to a collaborative work with mathematicians (which has benefited from this problem: solving the FK of a Gough platform is considered now as a classical bench in algebraic geometry). Although there are many mechanical architectures of parallel robots the FK problem for most of them may be reduced to solve the FK for a few key architectures.

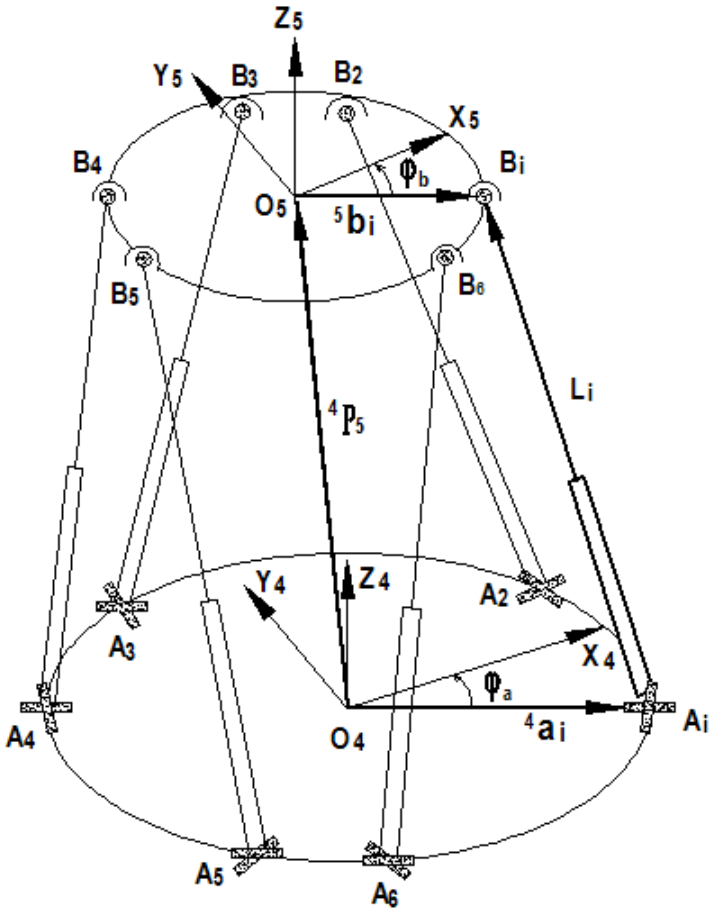

Figure 29. Norminal model of the Hexapod parallel mechanism

For real-time purpose many authors have proposed the use of the Newton-Raphson iterative scheme that assumes that an estimate of the solution is known. This scheme allows for possibly determining one solution of a non-linear square system of equations but there are many ways to model FK equations, not all of them being equivalent in term of quality of the result, computation time or size of the convergence domain. Furthermore, it is not so well known that the Newton scheme may converge toward a solution that is not the closest to the estimate, whatever closes is the estimate to this desired solution. Interval analysis based methods are good alternate with a similar computation time than Newton scheme and guarantee on the results. These methods share with the Newton scheme the possibility of a distributed implementation and we

believe that this opportunity must be used in a robot controller to speed up the FK which is essential for the control of the robot [54].

3.3.2 Inverse kinematics of the robot

1) For the carriage

According to the equations (12), (13) and (14), the inverse kinematic model can be obtained as:

$$\theta_4 = \sin^{-1}\left(\frac{p_x - d_3}{a_4}\right) \tag{15}$$

$$d_1 = p_z - a_3 c\theta_3 - a_4 c\theta_3 c\theta_4 \tag{16}$$

$$d_2 = -p_y - a_3 s\theta_3 - a_4 s\theta_3 c\theta_4 \tag{17}$$

2) For the Hexa-WH

The inverse kinematics of parallel robot is straightforward and easy to figure out compared with serial robot. According to the designed kinematic parameters, the following vector-loop equation represents the kinematics of the i^{th} limb of the manipulator

$$\overrightarrow{\mathbf{A}_i\mathbf{B}_i} = {}^4\mathbf{P}_5 + {}^4\mathbf{R}_5\,{}^5\mathbf{b}_i - {}^4\mathbf{a}_i \quad (i = 1,2,\cdots,6) \tag{18}$$

where ${}^4\mathbf{P}_5$ denotes the position vector of the task frame {5} with respect to the base frame {4}, and ${}^4\mathbf{R}_5$ is the Z-Y-X Euler transformation matrix expressing the orientation of the frame {5} relative to the frame {4},

$$ {}^{4}\mathbf{R}_{5} = \begin{bmatrix} c\alpha c\beta & c\alpha s\beta s\gamma - s\alpha c\gamma & c\alpha s\beta c\gamma + s\alpha s\gamma \\ s\alpha c\beta & s\alpha s\beta s\gamma + c\alpha c\lambda & s\alpha s\beta c\gamma - c\alpha s\gamma \\ -s\beta & c\beta s\gamma & c\beta c\gamma \end{bmatrix} \tag{19} $$

and the ${}^{4}\mathbf{a}_{i}$, ${}^{5}\mathbf{b}_{i}$ represent the position vectors of U-joints A_i and S-joints B_i in the coordinate frames {4} and {5} respectively

4 ERROR MODELLING AND ACCURACY ANALYSES OF IWR

In this section, the problem error modeling of the proposed IWR robot is discussed. Based on the vector differentiation method, the sensitivity model of the end-effector subject to the structure parameters is derived and analyzed. The relations between the position and orientation accuracy and manufacturing tolerances, actuation errors, and connection errors are formulated.

4.1 Introduction

Over the past decades, there have been a huge number of literatures are focused on the calibration of industrial robot and parallel robot. In what follows, we will first develop the error model of the carriage by using D-H convention based on the method proposed by W.K. Veitschegger and Chi-Haur Wu [29]. Then the error model of Hexa-WH and IWR are derived by using vector differentiation method. Last the computer simulations are performed to examine the validity and effectiveness of the error model.

4.2 Error modeling of carriage

For the accuracy of the carriage, it depends on the accuracy of the four-link parameters of each joint. If there are errors in the dimensional relationships between two consecutive joint $i-1$ and i , there will be a differential change $d\,{}^{i-1}\mathbf{A}_{i}$ between the two joint

coordinates. Therefore, the correct relationship between the two successive joint coordinates will be written as

$$ {}^{i-1}\mathbf{A}_i^c = {}^{i-1}\mathbf{A}_i + d\,{}^{i-1}\mathbf{A}_i \tag{20} $$

where ${}^{i-1}\mathbf{A}_i$ is the homogeneous matrix which have the nominal link parameters that can express the relationship between the joint coordinates $i-1$ and i, and $d\,{}^{i-1}\mathbf{A}_i$ is the differential change due to errors in the link parameters. It can be approximated as a linear function of four kinematic errors by Taylor's series:

$$ d\,{}^{i-1}\mathbf{A}_i = \frac{\partial {}^{i-1}\mathbf{A}_i}{\partial \theta_i}\Delta\theta_i + \frac{\partial {}^{i-1}\mathbf{A}_i}{\partial d_i}\Delta d_i + \frac{\partial {}^{i-1}\mathbf{A}_i}{\partial a_i}\Delta a_i + \frac{\partial {}^{i-1}\mathbf{A}_i}{\partial \alpha_i}\Delta\alpha_i \tag{21} $$

where $\Delta\theta_i, \Delta d_i, \Delta a_i$, and $\Delta\alpha_i$ are small errors in the kinematic parameters and the partial derivatives are evaluated with the nominal geometrical link parameters. From (1), taking the partial derivative with respect to θ_i, d_i, a_i, and α_i respectively， we can obtain

$$ \frac{\partial {}^{i-1}\mathbf{A}_i}{\partial \theta_i} = \begin{bmatrix} -s\theta_i & -c\theta_i \,\mathrm{c}\,\alpha_i & c\theta_i \,\mathrm{s}\,\alpha_i & -a_i s\theta_i \\ c\theta_i & -s\theta_i \,\mathrm{c}\,\alpha_i & s\theta_i \,\mathrm{s}\,\alpha_i & a_i c\theta_i \\ 0 & 0 & 0 & 0 \\ 0 & 0 & 0 & 0 \end{bmatrix} \tag{22} $$

$$ \frac{\partial {}^{i-1}\mathbf{A}_i}{\partial d_i} = \begin{bmatrix} 0 & 0 & 0 & 0 \\ 0 & 0 & 0 & 0 \\ 0 & 0 & 0 & 1 \\ 0 & 0 & 0 & 0 \end{bmatrix} \tag{23} $$

$$ \frac{\partial {}^{i-1}\mathbf{A}_i}{\partial a_i} = \begin{bmatrix} 0 & 0 & 0 & c\theta_i \\ 0 & 0 & 0 & s\theta_i \\ 0 & 0 & 0 & 0 \\ 0 & 0 & 0 & 0 \end{bmatrix} \tag{24} $$

$$\frac{\partial^{i-1}\mathbf{A}_i}{\partial\alpha_i}=\begin{bmatrix}0 & s\alpha_i s\theta_i & c\alpha_i s\theta_i & 0\\ 0 & -s\alpha_i c\theta_i & -c\alpha_i c\theta_i & 0\\ 0 & c\alpha_i & -s\alpha_i & 0\\ 0 & 0 & 0 & 0\end{bmatrix} \tag{25}$$

Let $d^{\,i-1}\mathbf{A}_i = {}^{i-1}\mathbf{A}_i * \delta^{\,i-1}\mathbf{A}_i$, and

$$\delta^{i-1}A_i = D_{\theta_i}\Delta\theta_i + D_{d_i}\Delta d_i + D_{a_i}\Delta a_i + D_{\alpha_i}\Delta\alpha_i \tag{26}$$

where $\mathbf{D}_{\theta_i}, \mathbf{D}_{d_i}, \mathbf{D}_{a_i}, \mathbf{D}_{\alpha_i}$ can be solved as follows:

$$\mathbf{D}_{\theta_i} = \left({}^{i-1}\mathbf{A}_i\right)^{-1} * \frac{\partial^{i-1}\mathbf{A}_i}{\partial\theta_i} = \begin{bmatrix}0 & -c\alpha_i & s\alpha_i & 0\\ c\alpha_i & 0 & 0 & a_i c\alpha_i\\ -s\alpha_i & 0 & 0 & -a_i s\alpha_i\\ 0 & 0 & 0 & 0\end{bmatrix} \tag{27}$$

$$\mathbf{D}_{d_i} = \left({}^{i-1}\mathbf{A}_i\right)^{-1} * \frac{\partial^{i-1}\mathbf{A}_i}{\partial d_i} = \begin{bmatrix}0 & 0 & 0 & 0\\ 0 & 0 & 0 & s\alpha_i\\ 0 & 0 & 0 & c\alpha_i\\ 0 & 0 & 0 & 0\end{bmatrix} \tag{28}$$

$$\mathbf{D}_{a_i} = \left({}^{i-1}\mathbf{A}_i\right)^{-1} * \frac{\partial^{i-1}\mathbf{A}_i}{\partial a_i} = \begin{bmatrix}0 & 0 & 0 & 1\\ 0 & 0 & 0 & 0\\ 0 & 0 & 0 & 0\\ 0 & 0 & 0 & 0\end{bmatrix} \tag{29}$$

$$\mathbf{D}_{\alpha_i} = \left({}^{i-1}\mathbf{A}_i\right)^{-1} * \frac{\partial^{i-1}\mathbf{A}_i}{\partial\alpha_i} = \begin{bmatrix}0 & 0 & 0 & 0\\ 0 & 0 & -1 & 0\\ 0 & 1 & 0 & 0\\ 0 & 0 & 0 & 0\end{bmatrix} \tag{30}$$

Substituting (27) through (30) into (26) and expanding it into matrix form we can obtain

$$\partial^{i-1}\mathbf{A}_i = \begin{bmatrix} 0 & -c\alpha_i\Delta\theta_i & s\alpha_i\Delta\theta_i & \Delta a_i \\ c\alpha_i\Delta\theta_i & 0 & -\Delta\alpha_i & a_i c\alpha_i\Delta\theta_i + s\alpha_i\Delta d_i \\ -s\alpha_i\Delta\theta_i & \Delta\alpha_i & 0 & -a_i s\alpha_i\Delta\theta_i + c\alpha_i\Delta d_i \\ 0 & 0 & 0 & 0 \end{bmatrix} \tag{31}$$

The above expression gives the differential translation and rotation vectors for any type of joint as functions of the four D-H kinematic errors. Similarly, for the proposed four degree-of-freedom carriage, the correct position and orientation of the task point p_4 with respect to the base frame due to the 4×4 kinematic errors can be expressed as

$${}^0\mathbf{A}_4^c = {}^0\mathbf{A}_4 + d\,{}^0\mathbf{A}_4 = \prod_{i=1}^{4}({}^{i-1}\mathbf{A}_i + d\,{}^{i-1}\mathbf{A}_i) \tag{32}$$

Expanding (32), and ignoring second and higher-order differential errors, then the relation between the differential change in carriage and the change in link parameters can be derived as

$$d\,{}^0\mathbf{A}_4 = \delta\mathbf{A}^1 * {}^0\mathbf{A}_4, \qquad \delta\mathbf{A}^1 = \sum_{i=1}^{4}([{}^0\mathbf{A}_i] * \delta^{i-1}\mathbf{A}_i * [{}^0\mathbf{A}_i]^{-1}) \tag{33}$$

where $\delta\mathbf{A}^1$ is the first order error matrix transformation in the fixed base frame, and

$$\delta^0\mathbf{A}_1 = \begin{bmatrix} 0 & 0 & \Delta\theta_1 & \Delta a_1 \\ 0 & 0 & -\Delta\alpha_1 & \Delta d_1 \\ -\Delta\theta_1 & \Delta\alpha_1 & 0 & -a_1\Delta\theta_1 \\ 0 & 0 & 0 & 0 \end{bmatrix} \tag{34}$$

$$\delta^1\mathbf{A}_2 = \begin{bmatrix} 0 & 0 & \Delta\theta_2 & \Delta a_2 \\ 0 & 0 & -\Delta\alpha_2 & \Delta d_2 \\ -\Delta\theta_2 & \Delta\alpha_2 & 0 & -a_2\Delta\theta_2 \\ 0 & 0 & 0 & 0 \end{bmatrix} \tag{35}$$

$$\delta^2\mathbf{A}_3 = \begin{bmatrix} 0 & 0 & \Delta\theta_3 & \Delta a_3 \\ 0 & 0 & -\Delta\alpha_3 & \Delta d_3 \\ -\Delta\theta_3 & \Delta\alpha_3 & 0 & -a_3\Delta\theta_3 \\ 0 & 0 & 0 & 0 \end{bmatrix} \tag{36}$$

$$\delta^3\mathbf{A}_4 = \begin{bmatrix} 0 & 0 & -\Delta\theta_4 & \Delta a_4 \\ 0 & 0 & -\Delta\alpha_4 & -\Delta d_4 \\ \Delta\theta_4 & \Delta\alpha_4 & 0 & a_4\Delta\theta_4 \\ 0 & 0 & 0 & 0 \end{bmatrix} \tag{37}$$

$${}^0\mathbf{A}_1 \cdot \delta^0\mathbf{A}_1 \cdot {}^0\mathbf{A}_1^{-1} = \begin{bmatrix} 0 & -\Delta\theta_1 & 0 & \Delta a_1 \\ \Delta\theta_1 & 0 & -\Delta\alpha_1 & d_1\Delta\alpha_1 \\ 0 & \Delta\alpha_1 & 0 & \Delta d_1 \\ 0 & 0 & 0 & 0 \end{bmatrix} \tag{38}$$

$${}^0\mathbf{A}_2 \cdot \delta^1\mathbf{A}_2 \cdot {}^0\mathbf{A}_2^{-1} = \begin{bmatrix} 0 & -\Delta\alpha_2 & -\Delta\theta_2 & -d_2\Delta\alpha_2 + d_1\Delta\theta_2 \\ \Delta\alpha_2 & 0 & 0 & -\Delta d_2 - a_1\Delta\alpha_2 \\ \Delta\theta_2 & 0 & 0 & \Delta a_2 - a_1\Delta\theta_2 \\ 0 & 0 & 0 & 0 \end{bmatrix} \tag{39}$$

${}^0\mathbf{A}_3 \cdot \delta^2\mathbf{A}_3 \cdot {}^0\mathbf{A}_3^{-1}$ and ${}^0\mathbf{A}_4 \cdot \delta^3\mathbf{A}_4 \cdot {}^0\mathbf{A}_4^{-1}$ can be obtained in the same way.

Following Paul [55], it can be seen that the above differential operators have the following form:

$$\delta T = \begin{bmatrix} 0 & -\delta\theta_z & \delta\theta_y & \delta d_x \\ \delta\theta_z & 0 & -\delta\theta_x & \delta d_y \\ -\delta\theta_y & \delta\theta_x & 0 & \delta d_z \\ 0 & 0 & 0 & 0 \end{bmatrix} \tag{40}$$

If let $\delta\mathbf{X}_0 = \begin{bmatrix} \delta d_x & \delta d_y & \delta d_z & \delta\theta_x & \delta\theta_y & \delta\theta_z \end{bmatrix}^T \in \Re^{6\times1}$ denote the positional and the orientation errors of the carriage, then compare (33) and (40), we can obtain the position and orientation errors of the end-effector of the carriage as

$$\delta\mathbf{X}_0 = \sum_{i=1}^{4} \Delta\mathbf{x}_i = \sum_{i=1}^{4} \left(\mathbf{G}_i \Delta y_i\right) \tag{41}$$

where $\Delta \mathbf{x}_i = \begin{bmatrix} \delta dx_i & \delta dy_i & \delta dz_i & \delta\theta x_i & \delta\theta y_i & \delta\theta z_i \end{bmatrix}^T$,and $\Delta \mathbf{y}_i = \begin{bmatrix} \Delta\theta_i & \Delta d_i & \Delta a_i & \Delta\alpha_i \end{bmatrix}^T$, $\mathbf{G}_i \in \Re^{6\times 4}$ is the identification Jacobian matrix. For example, from (38) and (39) we can get

$$\Delta \mathbf{x}_1 = \begin{bmatrix} \Delta a_1 \\ d_1 \Delta\alpha_1 \\ \Delta d_1 \\ \Delta\alpha_1 \\ 0 \\ \Delta\theta_1 \end{bmatrix} = \mathbf{G}_1 \mathbf{y}_1 = \begin{bmatrix} 0 & 0 & 1 & 0 \\ 0 & 0 & 0 & d_1 \\ 0 & 1 & 0 & 0 \\ 0 & 0 & 0 & 1 \\ 0 & 0 & 0 & 0 \\ 1 & 0 & 0 & 0 \end{bmatrix} \begin{bmatrix} \Delta\theta_1 \\ \Delta d_1 \\ \Delta a_1 \\ \Delta\alpha_1 \end{bmatrix} \tag{42}$$

$$\Delta \mathbf{x}_2 = \begin{bmatrix} -d_2\Delta\alpha_2 + d_1\Delta\theta_2 \\ -\Delta d_2 - a_1\Delta\alpha_2 \\ \Delta a_2 - a_1\Delta\theta_2 \\ 0 \\ -\Delta\theta_2 \\ \Delta\alpha_2 \end{bmatrix} = \mathbf{G}_2 \mathbf{y}_2 = \begin{bmatrix} d_1 & 0 & 0 & -d_2 \\ 0 & -1 & 0 & -a_1 \\ -a_1 & 0 & 1 & 0 \\ 0 & 0 & 0 & 0 \\ -1 & 0 & 0 & 0 \\ 0 & 0 & 0 & 1 \end{bmatrix} \begin{bmatrix} \Delta\theta_2 \\ \Delta d_2 \\ \Delta a_2 \\ \Delta\alpha_2 \end{bmatrix} \tag{43}$$

4.3 Error modeling of Hexa-WH

Let $\mathbf{l}_i$ be the unit vector in the direction of $\overrightarrow{A_iB_i}$, and l_i represents the magnitude of the leg vector $\overrightarrow{A_iB_i}$. Differentiating both sides of (18) will yield

$$\delta l_i \mathbf{l}_i + l_i \delta \mathbf{l}_i = \delta {}^4\mathbf{P}_5 + \delta {}^4\mathbf{R}_5 {}^5\mathbf{b}_i + {}^4\mathbf{R}_5 \delta {}^5\mathbf{b}_i - \delta {}^4\mathbf{a}_i. \text{ (i=1,2,...,6)} \tag{44}$$

Let ${}^4\mathbf{R}_5 {}^5\mathbf{b}_i = \mathbf{s}_i$, and multiply both sides of (44) with the unit direction vector $\mathbf{l}_i^T$, since $\mathbf{l}_i^T \mathbf{l}_i = 1, \mathbf{l}_i^T \delta \mathbf{l}_i = 0$ we can obtain:

$$\begin{aligned}\delta l_i &= \mathbf{l}_i^T \delta^4\mathbf{P}_5 + \mathbf{l}_i^T \delta^4\boldsymbol{\Omega}_5 \times \mathbf{s}_i + \mathbf{l}_i^{T\ 4}\mathbf{R}_5 \delta^5\mathbf{b}_i - \mathbf{l}_i^T \delta^4\mathbf{a}_i \\ &= \mathbf{l}_i^T \delta^4\mathbf{P}_5 + \left(\mathbf{s}_i \times \mathbf{l}_i\right)^{T\ 4}\boldsymbol{\Omega}_5 + \mathbf{l}_i^{T\ 4}\mathbf{R}_5 \delta^5\mathbf{b}_i - \mathbf{l}_i^T \delta^4\mathbf{a}_i \\ &= \begin{bmatrix}\mathbf{l}_i^T & \left(\mathbf{s}_i \times \mathbf{l}_i\right)^T\end{bmatrix}\begin{bmatrix}\delta^4\mathbf{P}_5 \\ \delta^4\boldsymbol{\Omega}_5\end{bmatrix} + \begin{bmatrix}-\mathbf{l}_i^T & \mathbf{l}_i^{T\ 4}\mathbf{R}_5\end{bmatrix}\begin{bmatrix}\delta^4\mathbf{a}_i \\ \delta^5\mathbf{b}_i\end{bmatrix}\end{aligned} \tag{45}$$

Equation (45) can be rewritten as

$$\delta\mathbf{L} = \mathbf{J}_1\delta\mathbf{X}_1 + \mathbf{J}_2\delta\mathbf{P}_1 \tag{46}$$

where

$$\delta\mathbf{L} = \left[\delta l_1, \delta l_2, \delta l_3, \delta l_4, \delta l_5, \delta l_6\right]^T \in \Re^{6\times 1} \tag{47}$$

$$\mathbf{J}_1 = \begin{bmatrix}\mathbf{l}_1^T & \left(\mathbf{s}_1 \times \mathbf{l}_1\right)^T \\ \vdots & \vdots \\ \mathbf{l}_6^T & \left(\mathbf{s}_6 \times \mathbf{l}_6\right)^T\end{bmatrix} \in \Re^{6\times 6} \tag{48}$$

$$\mathbf{J}_2 = \begin{bmatrix}\left(-\mathbf{l}_1^T & \mathbf{l}_1^{T\ 4}\mathbf{R}_5\right) & \cdots & 0 \\ \vdots & \ddots & \vdots \\ 0 & \cdots & \left(-\mathbf{l}_6^T & \mathbf{l}_6^{T\ 4}\mathbf{R}_5\right)\end{bmatrix} \in \Re^{6\times 36} \tag{49}$$

and

$$\delta\mathbf{P}_1 = \begin{bmatrix}\delta^4\mathbf{a}_i & \delta^5\mathbf{b}_i\end{bmatrix}^T \in \Re^{36\times 1} \quad \iota=1,2,...,6 \tag{50}$$

Since $\mathbf{J}_1 \in \Re^{6\times 6}$ is a square matrix, and no singular points exist inside the workspace, $\mathbf{J}_1$ is invertible. Therefore, (46) can be written as:

$$\delta\mathbf{X}_1 = \mathbf{J}_1^{-1}\delta\mathbf{L} - \mathbf{J}_1^{-1}\mathbf{J}_2\delta\mathbf{P}_1 \tag{51}$$

The first term on the right side represents the errors induced by actuators and the second one is the position errors from the passive joints A_i and B_i.

4.4 Error modeling of IWR

The schematic diagram of the redundant hybrid manipulator is shown in Figure 30, which is a combination of carriage and Hexapod manipulator mentioned above. The base plate frame {4} of Hexapod is coincided with the end task frame of the carriage. The global base frame {0} is located at the left rail.

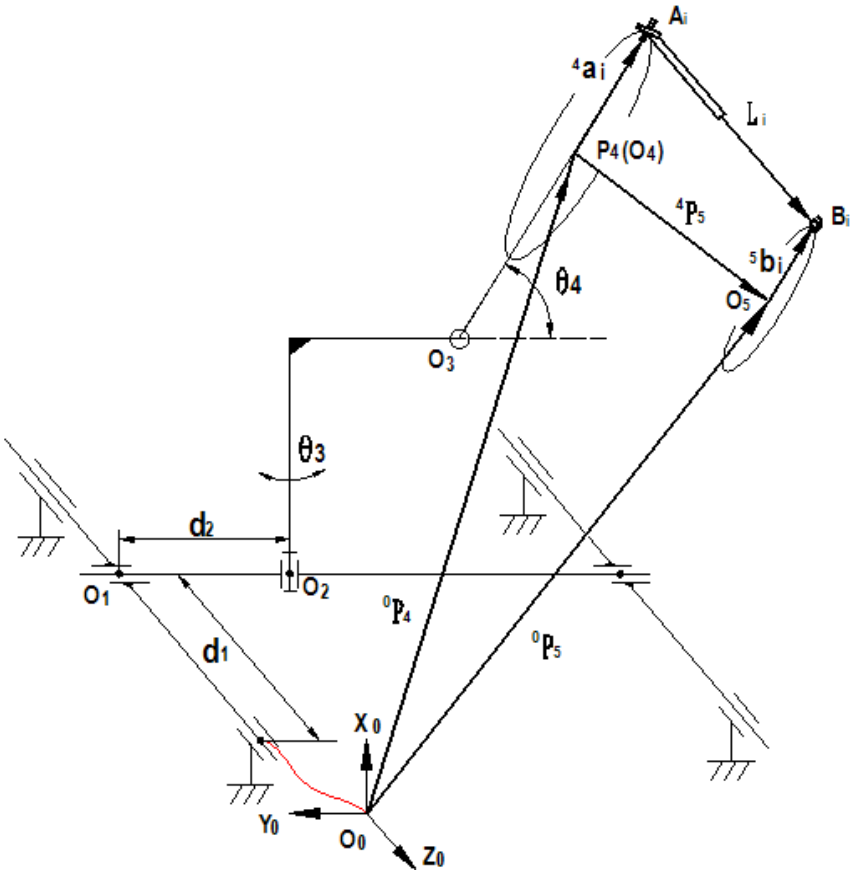

Figure 30. Schematic diagram of IWR

According to the geometry, a vector-loop equation can be derived as

$$
\begin{aligned}
{}^{0}\mathbf{P}_5 &= {}^{0}\mathbf{P}_4 + {}^{0}\mathbf{R}_4\,{}^{4}\mathbf{P}_5 = {}^{0}\mathbf{P}_4 + {}^{0}\mathbf{R}_4({}^{4}\mathbf{a}_i - {}^{4}\mathbf{R}_5\,{}^{5}\mathbf{b}_i) \\
&= {}^{0}\mathbf{P}_4 + {}^{0}\mathbf{R}_4 l_i \mathbf{l}_i + {}^{0}\mathbf{R}_4\,{}^{4}\mathbf{a}_i - {}^{0}\mathbf{R}_5\,{}^{5}\mathbf{b}_i
\end{aligned}
\tag{52}
$$

where ${}^0\mathbf{P}_5$ is the position vector of the task frame {5} (or end-effector) with respect to the fixed base frame {0}, and ${}^0\mathbf{R}_4$ is the rotation matrix of the frame {4} with respect to frame {0}.

Differentiating both sides of (52) and multiplying unit direction vector $\mathbf{l}_i^T$ yields

$$\begin{bmatrix} \mathbf{l}_i^T & (\mathbf{r}_{bi} \times \mathbf{l}_i)^T \end{bmatrix} \begin{bmatrix} \delta {}^0\mathbf{P}_5 \\ \delta {}^0\boldsymbol{\Omega}_5 \end{bmatrix} = \begin{bmatrix} \mathbf{l}_i^T & (\mathbf{r}_{ai} \times \mathbf{l}_i)^T + ({}^0\mathbf{R}_4 l_i \mathbf{l}_i \times \mathbf{l}_i)^T \end{bmatrix} \begin{bmatrix} \delta {}^0\mathbf{P}_4 \\ \delta {}^0\boldsymbol{\Omega}_4 \end{bmatrix}$$
$$+ \mathbf{l}_i^T {}^0\mathbf{R}_4 \mathbf{l}_i \delta l_i + \begin{bmatrix} \mathbf{l}_i^T {}^0\mathbf{R}_4 & -\mathbf{l}_i^T {}^0\mathbf{R}_5 \end{bmatrix} \begin{bmatrix} \delta {}^5\mathbf{a}_i \\ \delta {}^4\mathbf{b}_i \end{bmatrix} \tag{53}$$

where $\mathbf{r}_{bi} = {}^0\mathbf{R}_5 {}^5\mathbf{b}_i$, $\mathbf{r}_{ai} = {}^0\mathbf{R}_4 {}^4\mathbf{a}_i$

Equation (53) can be rewritten as

$$\mathbf{J}_3 \delta \mathbf{X} = \mathbf{J}_4 \delta \mathbf{X}_0 + \mathbf{J}_5 \delta \mathbf{L} + \mathbf{J}_6 \delta \mathbf{P}_1 \tag{54}$$

where

$$\mathbf{J}_3 = \begin{bmatrix} \mathbf{l}_1^T & (\mathbf{r}_{b1} \times \mathbf{l}_1)^T \\ \vdots & \vdots \\ \mathbf{l}_6^T & (\mathbf{r}_{b6} \times \mathbf{l}_6)^T \end{bmatrix} \in \Re^{6\times 6} \tag{55}$$

$$\mathbf{J}_4 = \begin{bmatrix} \mathbf{l}_1^T & (\mathbf{r}_{a1} \times \mathbf{l}_1)^T + (l_i {}^0\mathbf{R}_4 \mathbf{l}_1 \times \mathbf{l}_1)^T \\ \vdots & \vdots \\ \mathbf{l}_6^T & (\mathbf{r}_{a6} \times \mathbf{l}_6)^T + (l_i {}^0\mathbf{R}_4 \mathbf{l}_6 \times \mathbf{l}_6)^T \end{bmatrix} \in \Re^{6\times 6} \tag{56}$$

$$\mathbf{J}_5 = \begin{bmatrix} \mathbf{l}_1^T {}^0\mathbf{R}_4 \mathbf{l}_1 & \cdots & 0 \\ \vdots & \ddots & \vdots \\ 0 & \cdots & \mathbf{l}_6^T {}^0\mathbf{R}_4 \mathbf{l}_6 \end{bmatrix} \in \Re^{6\times 6} \tag{57}$$

$$\mathbf{J}_6 = \begin{bmatrix} (\mathbf{l}_1^T {}^0\mathbf{R}_4 & -\mathbf{l}_1^T {}^0\mathbf{R}_5) & \cdots & 0 \\ \vdots & & \ddots & \vdots \\ 0 & & \cdots & (\mathbf{l}_6^T {}^0\mathbf{R}_4 & -\mathbf{l}_6^T {}^0\mathbf{R}_5) \end{bmatrix} \in \Re^{6\times 36} \tag{58}$$

Since $\mathbf{J}_3 \in \Re^{6\times6}$ is a square matrix, and no singular points exist inside the workspace, $\mathbf{J}_3$ is invertible. Therefore, (55) can be rewritten as:

$$\delta\mathbf{X} = \mathbf{J}_3^{-1}\mathbf{J}_4\delta\mathbf{X}_0 + \mathbf{J}_3^{-1}\mathbf{J}_5\delta\mathbf{L} + \mathbf{J}_3^{-1}\mathbf{J}_6\delta\mathbf{P}_1 \tag{59}$$

where $\delta\mathbf{X} = \begin{bmatrix} \delta^0\mathbf{P}_5 & \delta^0\boldsymbol{\Omega}_5 \end{bmatrix}^T \in \Re^{6\times1}$ denote the final output pose errors, and the first term on the right is the errors caused by the carriage, the second and third one represent the errors induced by the Hexapod mechanism.

4.5 Simulation results

In order to evaluate the final output errors caused by the error sources, a simulation example was performed using the following nominal parameters.

$$\left|{}^4\mathbf{a}_i\right| = 328mm, \left|{}^5\mathbf{b}_i\right| = 130mm, a_1 = 91mm, a_2 = 0,$$
$$a_3 = 252mm, a_4 = 354mm; d_3 = 331mm, d_4 = 0$$

Moreover, to estimate the accuracy of the derived error model, we assume a certain kinematic errors occurred in the carriage and Hexapod

$$\left|\delta\mathbf{L}\right| = 0.5mm, \left|\delta\mathbf{P}_1\right| = 0.1mm$$
$$\left|\Delta\alpha_i\right| = \left|\Delta\theta_i\right| = 0.1^\circ; \left|\Delta a_i\right| = \left|\Delta d_i\right| = 0.5mm$$

The range of the actuator input values are given in below, which will be generated by the random function in Matlab. The output position errors and orientation errors of the carriage, Hexapod and the whole robot in X, Y and Z direction for the 40 random generated poses are shown in Figure 31-36 respectively. Figure 37 and Figure 38 illustrate the comparison of the absolute position and orientation error of carriage, Hexapod and the whole robot.

$$0 < d_1 < 800mm, 0 < d_2 < 300mm, 0^\circ < \theta_3 < 180^\circ,$$
$$0^\circ < \theta_4 < 90^\circ, 0^\circ < \alpha < 15^\circ, 0^\circ < \beta < 15^\circ, 0^\circ < \gamma < 10^\circ.$$

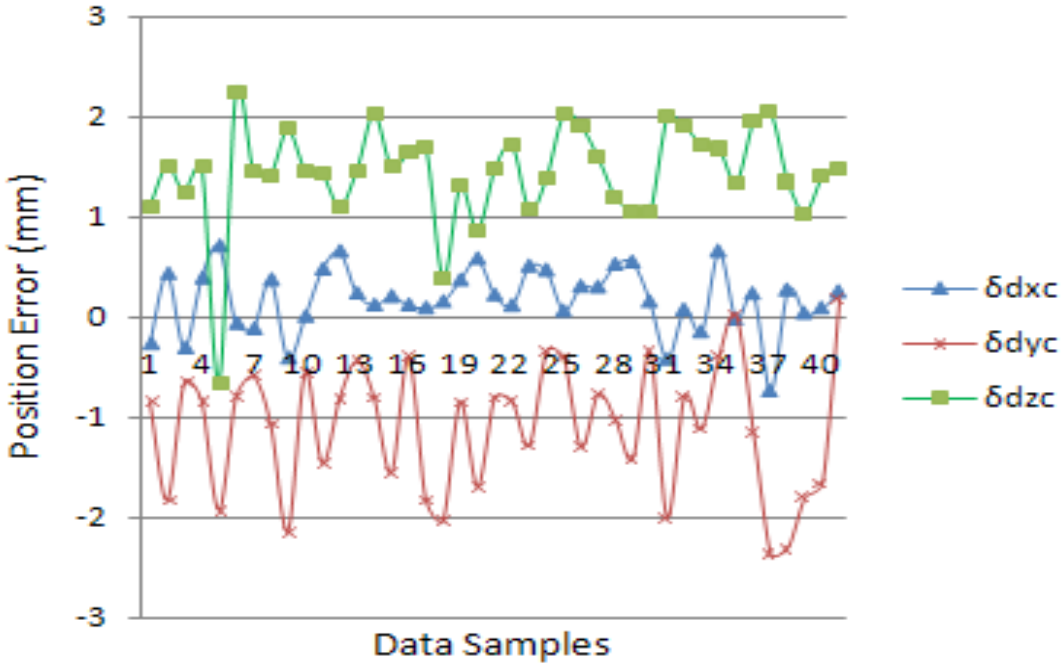

Figure 31. Position error of carriage in X, Y, and Z

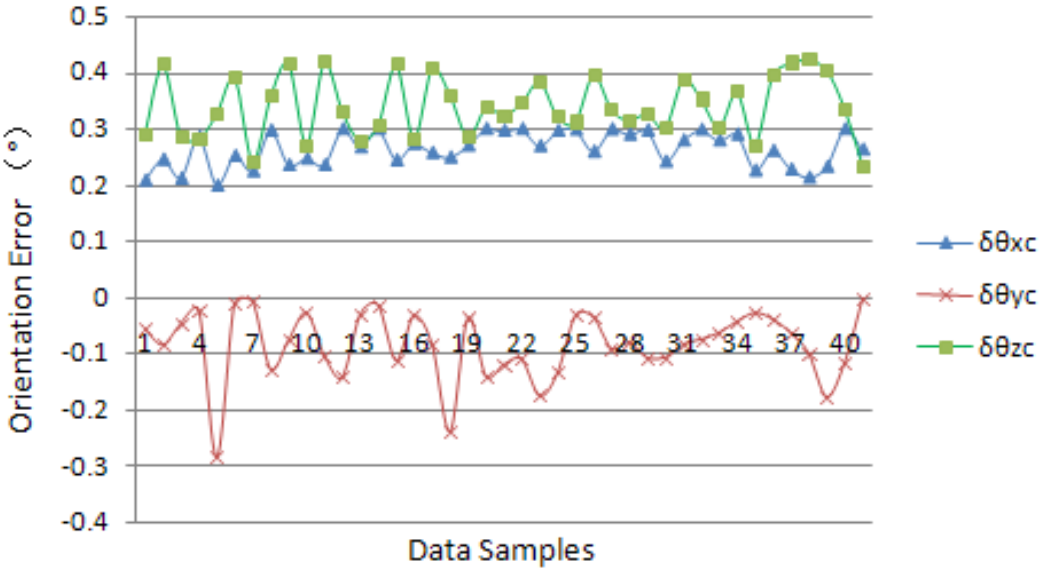

Figure 32. Orientation error of carriage in X, Y, and Z

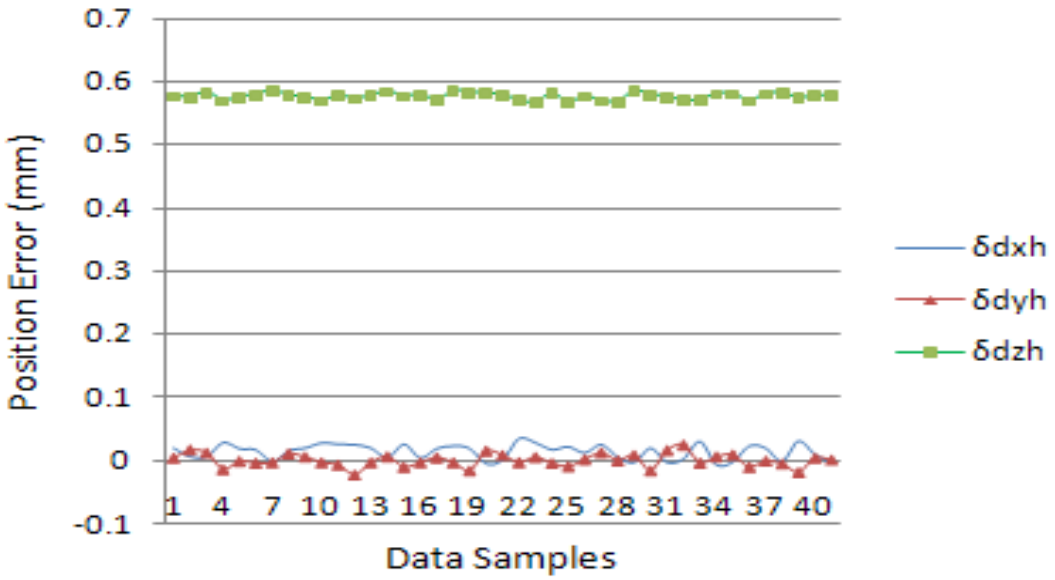

Figure 33. Position error of Hexapod in X, Y, and Z

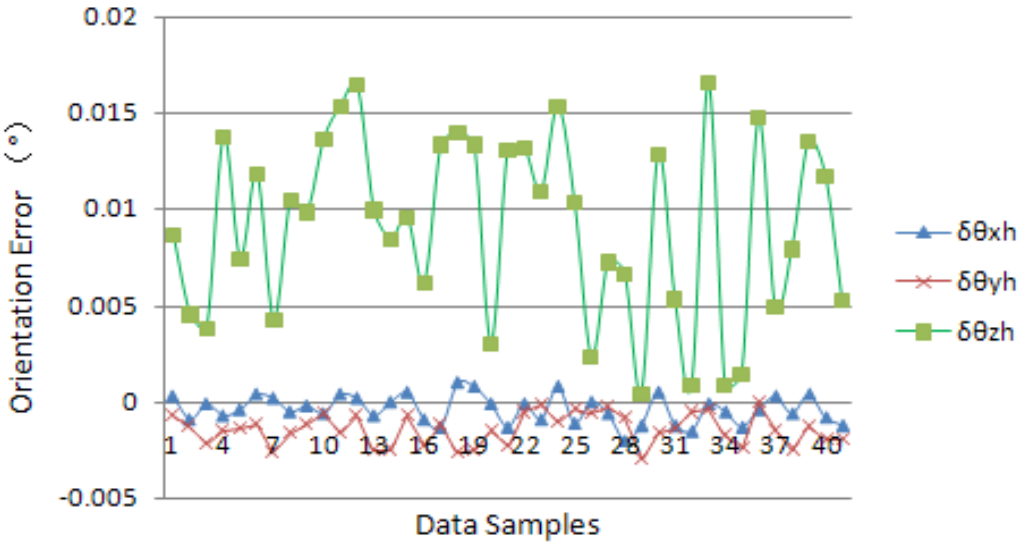

Figure 34. Orientation error of Hexapod in X, Y, and Z

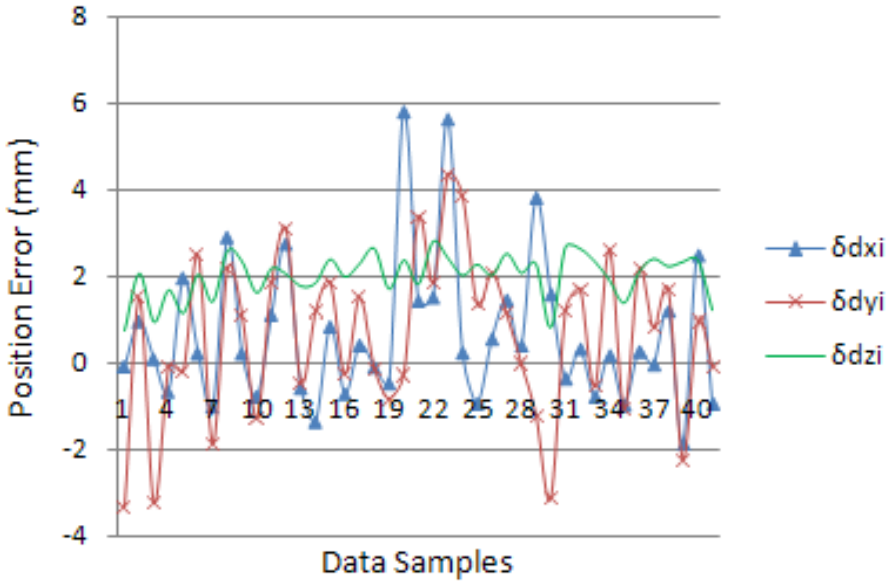

Figure 35. Position error of IWR in X, Y, and Z

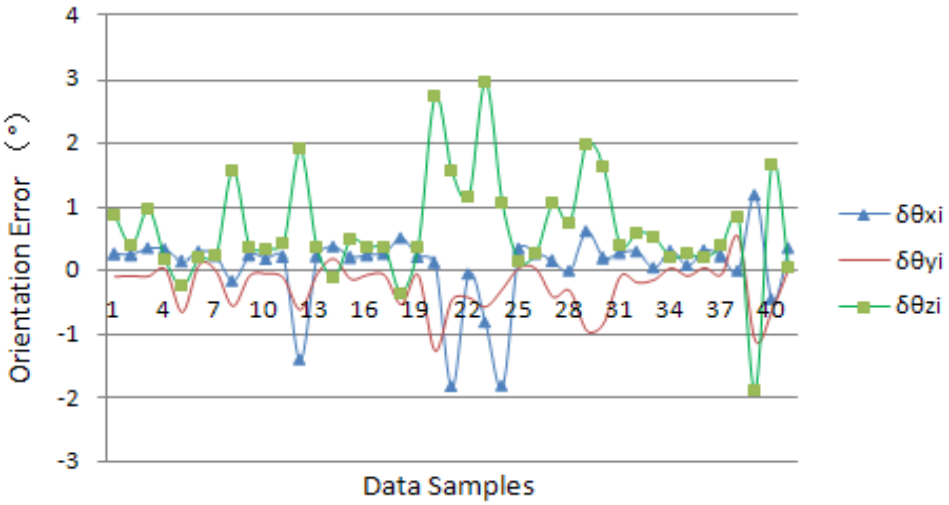

Figure 36. Orientation error of IWR in X, Y, and Z

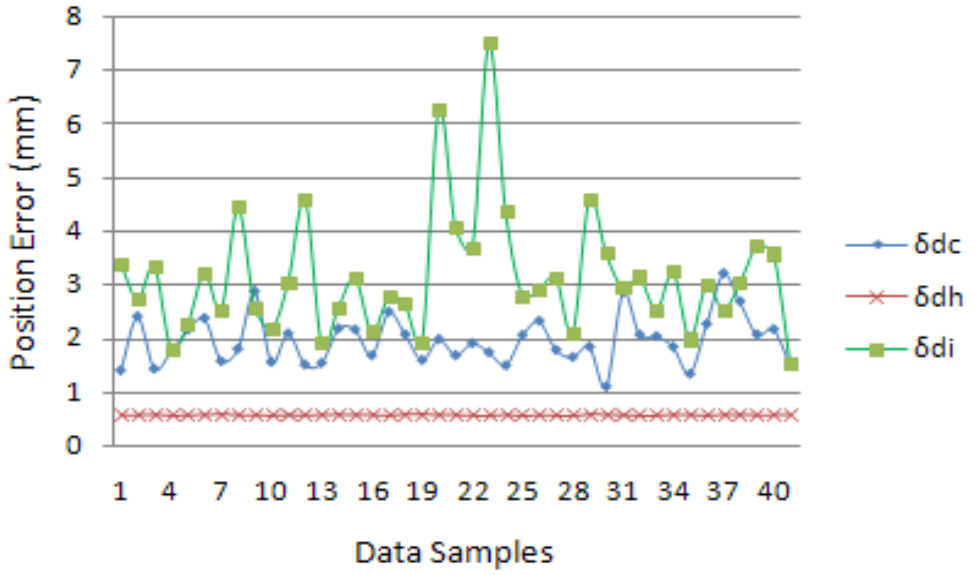

Figure 37. Comparison of the absolute position error of carriage, Hexapod and IWR

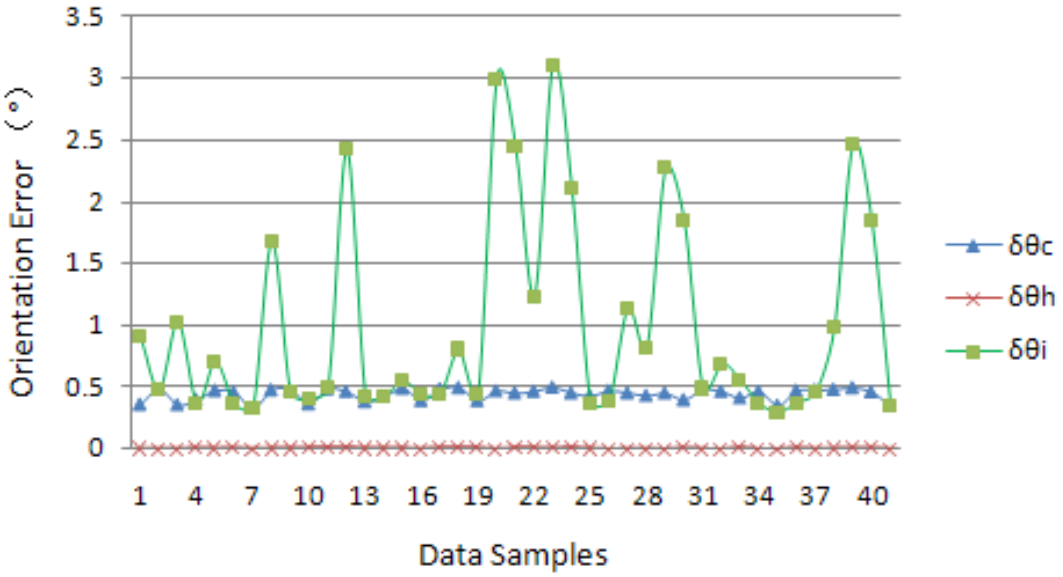

Figure 38. Comparison of the absolute orientation error of carriage, Hexapod and IWR

From these Figures it can be seen that the errors along Z axis are influenced significantly than that of X, Y axes, and the final output errors are not simply the superposition of the carriage and Hexapod. Comparing the absolute position and orientation errors of the carriage, Hexapod and IWR, we can see that the carriage error is the most important error sources to the final output errors, which causes about 80% of the whole errors. The final

position errors are not greater than 10mm, which can be reduced to satisfy the accuracy requirement by means of some calibration methods in next step.

5 CONCLUSIONS

In this paper, a hybrid redundant robot IWR which used for both machining and assembling of Vacuum Vessel of ITER is introduced. An error model derived for the proposed robot has the ability to account for the static sources of errors. Due to its complex structure and 4 redundant degrees of freedom, we divide the robot into serial part and parallel one, and then formulate the error model respectively, finally combine them together to get the final error model.

The thesis also presents a general overview of the art of the date robot calibration methods and existing error analysis methods for pure serial and parallel robot. Then take the studied robot as an example, the kinematics of the robot was analyzed. The forward and inverse kinematics of the robot was derived. Finally, the error models for the carriage, Hexa-WH and the whole robot was given based on the differential algorithm method.

To validate the effectiveness of our developed error model, the computer simulation was performed in Matlab based on the derived error model and the results show that about 80% amount of errors in the end-effector is caused by serial link mechanism, i.e. carriage. The final position errors are not greater than 10mm. In practice, to obtain desired accuracy of robot, these errors have to be reduced by further parameter identification methods.

In the following work, efforts will be focused on the parameter identification by using some optimization methods to obtain desirable output errors.

REFERENCES

[1] Huapeng Wu, Heikki Handroos, Pekka Pessi, Juha Kilkki, Lawrence Jones, "Development and control towards a parallel water hydraulic weld/cut for machining processes in ITER vacuum vessel". Int. J. fusion Engineering and Design, Vol. 75-79, pp. 625-631, 2005.

[2] Webpage: "http://www.iter.org/a/index_nav_1.htm", (retrieved May 15, 2008).

[3] A.Y.Elatta, Li Pei Gen,Fan liang Zhi et al, "An Overview of Robot Calibration", Information Technology Journal 3 (1): pp.74-78,2004

[4] Edited by R.Bernhardt, S.L.Albright, "Robot Calibration". Chapman and Hall , London,1993

[5] Fazenda, N., "Calibration of High-Precision Flexure Parallel Robots", Thèse No 3712 (PhD dissertation), École Polytechnique Fédérale de Lausanne, 2006.

[6] J. M. Hollerbach, "A Survey of Kinematic Calibration", In Robotics Review, O. Khatib, J. J. Craig and T. Lozano-Perez (editors), MIT Press, 1988.

[7] M. Vincze, K. M. Filz, H. Gander, J. P. Prenninger and G. Zeichen, "A Systematic Approach to Model Arbitrary Non Geometric Kinematic Errors", In Advances in robot kinematics and computational geometry, J. Lenarcic and B. Ravani (editors), pp 129 – 138, 1994.

[8] Chunhe Gong, Jingxia Yuan, Jun Ni, "Nongeometric error identification and compensation for robotic system by inverse calibration", International Journal of Machine Tools &Manufacture, Vol.40, pp.2119-2137, 2000.

[9] L. J. Everett, "Models for diagnosing robot error sources", Proceedings of the IEEE Conference on Robotics and Automation, Vol. 2, pp 155 – 159, May 1993.

[10] Marco A. Meggiolaro, Steven Dubowsky, Constantinos Mavroidis, "geometric and elastic error calibration of a high accuracy patient positioning system", Mechanism and Machine Theory 40, pp.415-427, 2005.

[11] Yu Liu, Bin Liang,Cheng Li, Lijun Xue, Songhua Hu, "Calibration of a Stewart Parallel Robot using genetic Algorithm", Proceedings of the 2007 IEEE International Conference on Mechantronics and Automation, pp.2495-2500, Harbin, China, August ,2008

[12] J. M. Lewis, X. L. Zhong and H. Rea, "A neural network approach to the robot inverse calibration problem", Proceedings of the IEE International Conference on Intelligent Systems Engineering, pp 342 – 347, September 1994.

[13] J. M. Hollerbach and C. W. Wampler, "The calibration index and taxonomy for robot kinematic calibration methods", International Journal of Robotics Research, Vol. 15, Issue 6, pp. 573 – 591, 1996.

[14] J. W. Jeong, S. H. Kim, Y. K. Kwak and C. C. Smith, "Development of a parallel wire mechanism for measuring position and orientation of a robot end-effector", Mechatronics, Vol. 8, pp. 845 – 861, 1998.

[15] A. Goswami, A. Quaid and M. Peshkin, "Complete parameter identification of a robot from partial pose information", Proceedings of the IEEE International Conference on Robotics and Automation, pp.168 – 173, May 1993.

[16] G. Alici and B. Shirinzadeh, "Laser Interferometry Based Robot Position Error Modelling for Kinematic Calibration", Proceedings of the IEEE International Conference on Intelligent Robots and Systems, Las Vegas – Nevada (USA), pp 3588 – 3593, October 2003.

[17] G.-R. Tang and L.-S. Liu, "Robot calibration using a single laser displacement meter", Mechatronics, Vol. 3, No. 4, pp. 503 – 516, 1993.

[18] J. O. Berg, "Path and Orientation Accuracy of Industrial Robots", International Journal of Advanced Manufacturing Technology, Vol. 8, pp. 29 – 33, Springer – Verlag, 1993.

[19] W. S. Newman, C. E. Birkhimer and R. J. Horning, "Calibration of a Motoman P8 Robot Based on Laser Tracking", Proceedings of the IEEE International Conference on Robotics and Automation, San Francisco – California (USA), Vol. 4, pp 3597 – 3602, April 2000.

[20] Y. Bai, H. Zhuang and Z. S. Roth "Experiment Study of PUMA Robot Calibration Using a Laser Tracking System", Proceedings of the IEEE International Workshop on Soft Computing in Industrial Applications, Binghamton – New York (USA), pp 139 – 144, June 2003.

[21] H. Zhuang, "Camera-Aided Robot Calibration", CRC Press, 1996.

[22] H. Zhuang, O. Masory, J. Yan, "Kinematic Calibration of a Stewart Platform Using Pose Measurements Obtained by a Single Theodolite", Proceedings of the IEEE/RSJ International conference on Intelligent Robots and Systems, Vol. 2, pp 329 – 334, August 1995.

[23] S. Besnard and W. Khalil, "Calibration of parallel robots using two inclinometers", Proceedings of the IEEE International Conference on Robotics and Automation, pp 1758 – 1763, Detroit – Michigan (USA), May 1999.

[24] Ota, H., Shibukawa,T., Tooyama, T. and Uchiyama, M., "Forwad Kinematic Calibration Method for Parallel Mechanism Using Pose Data Measured by a Double Ball Bar System", Proceedings of the Year 2000 Parallel Kinematic Mechines International Conference, pp.57-62. 2000.

[25]Webpage:
"http://www.optics.arizona.edu/opti696/2006/StudentPresentations/Laser%20Tracker%20Presentation.pdf", (retrieved June 10, 2008).

[26]Webpage:
"http://www.space.com/scienceastronomy/astronomy/interferometry_101.html", (retrieved June 3, 2008).

[27] Webpage: "http://www.renishaw.com/en/6813.aspx ", (retrieved June21, 2008).

[28] C. H. Wu, "A kinematic CAD tool for the design and control of robot manipulators," Int. J. Robotics Res., vol. 3, no. 1, pp. 58-67, Spring 1984.

[29] W.K. Veitschegger, Chi-Haur Wu, "Robot analysis based on kinematics". IEEE J. Robotics and Automation, Vol. RA-2,NO.3, pp. 171-179, september, 1986.

[30] W. Khalil and M. Gautier, "Calculation of the identifiable parameters for robots calibration," in 9th IFACLFOR Symp. on Identi. and Sys. Parameter Estimation, Budapest, Hungaria, pp.888-892,1991.

[31] J.-H. Borm and C.-H. Menq, "Experimental study of observability of parameter errors in robot calibration", Proceedings of the IEEE International Conference on Robotics and Automation, Vol. 1, pp 587 – 592, May 1989.

[32] David Daney, "Identification of parallel robot kinematic parameters", Proceedings of the 11th World Congress in Mechanism and Machine Science, China, April, 2004.

[33] Lung-Wen Tsai,"Robot Analysis- the Mechanics of Serial and Parallel Manipulators". Wiley & Sons, New York, 2000.

[34] Webpage: "http://prime.jsc.nasa.gov/ROV/types.html", (retrieved June 15, 2008).

[35] Roth Z, Benjamin W. Mooring, Bahram ravani, "An overview of Robot Calibration". IEEE Journal of Robotics and Automation. Vol. Ra-3.No.5, Oct. 1987.

[36]Webpage:
"http://en.wikipedia.org/wiki/Robot_calibration#Accuracy_criteria_and_error_sources", (retrieved June 15, 2008).

[37] J. Craig, "Introduction to Robotics: Mechanics and Control", Addison-Wesley Publishing Co., Reading, MA, 1986.

[38] S. Hayati, "Robot Arm Geometric Link Parameter Estimation", Proceedings of the 22nd Conference of the IEEE Control Systems Society, Decision and Control, San Antonio – Texas (USA), Vol. 3, pp. 1477 – 1483, December 1983.

[39] P.S.Shiakolas, K.L.Conrad, and T.C.Yih, "On the Accuracy, Repeatability, and Degree of Influence of Kinematics Parameters for Industrial Robots", Int.J of Modeling and Simulation, Vol.22.No.3,2002.

[40] Stone, H.W. and Sanderson, A.C. "A Prototype Arm Signature Identification System", In the Proceedings of the IEEE International Conference on Robotics and Automation, pp. 175-182, 1987.

[41] Takeda, Y., Shen, G. and Funabashi, H., "A DBB-Based Kinematic calibration Method for in-parallel Actuated Mechanisms Using a Fourier Series", Proceedings of DETC'02, ASME 2002 Design Engineering Technical Conferences and

Computer and Information in Engineering Conference, DETC2002/MECH 34345, pp.1-10, 2002.

[42] Y. Koseki, T. Arai, K. Sugimoto, T. Takatuji and M. Goto, "Design and accuracy evaluation of high speed precision parallel mechanism", Proceedings of the IEEE International Conference on Robotics and Automation, pp 1340 – 1345, Leuven (Belgium), May 1998.

[43] L. J. Everett and T. W. Ives, "A sensor used for measurements in the calibration of production robots", Proceedings of the IEEE Conference on Robotics and Automation, pp 174 – 179, Atlanta – Georgia (USA), May 1993.

[44] A. Nahvi, J. M. Hollerbach and V. Hayward, "Calibration of a Parallel Robot Using Multiple Kinematic Closed Loops", Proceedings of the IEEE International Conference Robotics and Automation (ICRA), Vol. 1, pp 407 – 412, May 1994.

[45] C. W. Wampler, J. M. Hollerbach and T. Arai, "An Implicit Loop Method for Kinematic Calibration and Its Application to Closed-Chain Mechanisms", IEEE Transactions on Robotics and Automation, Vol. 11, No. 5, pp 710 – 724, October 1995.

[46] M. Abderrahim and A. R. Whittaker, "Kinematic model identification of industrial manipulators", Robotics and Computer-Integrated Manufacturing Vol. 16, pp 1 – 8, 2000.

[47] H. Zhuang and L. Liu, "Self calibration of a class of parallel manipulators," in Proc. IEEE Int. Conf. Robot. Automat. Minneapolis, MN, 1996, pp. 994–999.

[48] Gael Ecorchard and Patrick Maurine, "Self-Calibration of Delta Parallel Robots with Elastic Deformation Compensation", Proceedings of the IEEE International Conference on Intelligent robots and System, pp. 1283- 1288,Aug. 2005.

[49] Khalil W. and Besnard S. "Self calibration of Stewart-Gough parallel robot without extra sensors". IEEE Trans. on Robotics and Automation, 15(6): pp. 1116–1121, December 1999.

[50] K. Han, W. Chung, and Y. Youm, "Local structurization for the forward kinematics of parallel manipulators using extra sensor data," in Proc. IEEE Int. Conf. Robot. Automat, pp. 514–520, Nagoya, Japan, 1995.

[51] J. P. Merlet, "Closed-form resolution of the direct kinematics of parallel manipulators using extra sensors data," in Proc. IEEE Int. Conf. Robot. Automat., pp. 200–204, Atlanta, GA, 1993.

[52] J. P. Merlet, "Parallel Robots", (Second Edition).Published by Springer, Netherlands, 2006.

[53] Webpage: "http://en.wikipedia.org/wiki/Robot_kinematics",(retrieved July21, 2008).

[54] Webpage:

"http://www-sop.inria.fr/members/Jean-Pierre.Merlet//ASME/asme2002.html", (retrieved July 21, 2008).

[55] R.P.Paul, Robot Manipulators:Mathematics, Programming, and Control, The MIT Press, Cambridge, MA, 1982.